

**NULL DEPTH TRADE OFF
FOR OUTPUT POWER REDUCTION IN A
DOWNLINK ADAPTIVE ANTENNA ARRAY**

By

TUAN NGUYEN

SUBMITTED IN FULFILLMENT OF THE REQUIREMENT FOR THE DEGREE OF:

MASTER OF ENGINEERING

AT

VICTORIA UNIVERSITY OF TECHNOLOGY

MELBOURNE, AUSTRALIA

2006

Declaration

“I, TUAN ANH NGUYEN, declare that the Master by Research thesis entitled NULL DEPTH TRADE OFF FOR OUTPUT POWER REDUCTION IN A DOWNLINK ADAPTIVE ANTENNA ARRAY is no more than 60,000 words in length, exclusive of tables, figures, appendices, references and footnotes. This thesis contains no material that has been submitted previously, in whole or in part, for the award of any other academic degree or diploma. Except where otherwise indicated, this thesis is my own work”.

Signature:

Date:

Acknowledgment

I would like to express my gratitude to Professor Mike Faulkner of Telecommunications and Microelectronics Group (T μ E), Victoria University of Technology of Australia (VUT) for his invaluable advices and encouragements. Without his guidance, this thesis would be impossible. I also want to thank Dr Reza Berangi, who gave me many encouragements and useful discussions during my difficult time of seeking the direction of research. My gratitude also goes to all staff members, my fellow research students for open discussions and technical assistances when it was necessary.

Last but not least, I want to thank my wife for her patience and support during all my long study years. I also thank my children for their loves and thoughtfulness.

Abstract

The zero-forcing algorithm (*min-norm* algorithm) is one of the proposed methods for downlink beamforming. This algorithm steers the nulls towards interferers and the main beam towards the desired user provided the angles of arrival of these signals are known to the base station. However, downlink adaptive arrays use additional power when they are required to include null steering in their beam patterns. This excessive transmitted power reduces the effective antenna gain, increases interference in other directions and has implications on the dimensioning of the power amplifiers feeding the antenna elements. In addition, the power distribution among the antenna array elements is no longer equal. The design ratings for the power amplifiers (PAs) on each element can differ by up to 2.9 dB. A distributed amplifier design could solve this problem. This thesis investigates the trade-off of null depth with transmitted power and utility by modifying the zero-forcing algorithm. The performance or utility of the antenna is defined here as the probability that it can accommodate a given angular scenario between the desired user and interfering sources without transmitting excessive power. A -10 dB null increases antenna utility by 6% when steering a single null and 17% when steering 2 nulls if the excessive transmit power is held below 3 dB for a 4-element antenna array. In this work, a modified version of the min-norm algorithm was used to design the antenna weights from angle of arrival information.

Table of Contents

1	<i>Introduction.....</i>	12
2	<i>Motivation and Background</i>	14
2.1	Motivation.....	14
2.2	Problem statement	16
2.3	Adaptive Antenna Array Principle	19
2.3.1	Uniform Linear Array (ULA)	19
2.3.2	Uplink and Downlink Channel Model	23
2.4	Antenna array simulator	29
2.4.1	Study of the variation of the antenna array beam patterns.....	29
2.4.2	Basic antenna array simulator	29
2.4.3	Plotting antenna array radiation pattern	32
2.4.4	Analysis the error effect by antenna simulator	33
2.4.5	Simulation of adaptation process	35
2.5	Adaptive Beamforming Algorithms	36
2.5.1	Survey of previous work.....	36
2.5.2	Beamforming techniques	37
2.5.3	DOA estimation algorithms	40
2.5.4	The MUSIC Algorithm	44
2.5.5	Selection of downlink adaptive algorithms.....	47
2.5.6	A "difficult" situation for the adaptive array	49
3	<i>Novel beamforming criterion.....</i>	51
3.1	Observation of output power increasing when separation angle is small...51	

3.2	Zero-forcing beamformer	53
3.3	Output power reduction by changing the null depth	55
3.3.1	Global minimum of the output power surface	55
3.3.2	Minimum of the output power by varying ϕ	57
3.3.3	Algorithm for output power reduction by trading off the null depth.....	61
4	<i>Numerical verification and simulation results</i>	64
4.1	Trade off null depth for the output power reduction	64
4.2	Power constraints for a linear array	64
4.3	Additional transmit power for null steering.....	67
4.4	Power distribution between the antenna elements	68
4.4.1	Scenario of one user and one interferer	68
4.4.2	Scenario of one user and two interferers.....	71
5	<i>Conclusion.....</i>	76
6	<i>Summary Of Significance.....</i>	78

List of Figures

Figure 1 The four- element antenna array radiation pattern (in dB scale).....	17
Figure 2 The nine- element antenna array radiation pattern (in dB scale).....	17
Figure 3 An ULA with plane wave arrives at angle θ	21
Figure 4 Uplink: the base station receives signals and multipath copies from mobiles.	25
Figure 5 Downlink: the base station transmits signals to co-channel users.....	28
Figure 6 Basic Antenna Array Simulator GUI	31
Figure 7 By changing a few factors, the antenna simulator can display the variation of the radiation pattern. This feature can be used to predict behaviour of the array under effect of error or disturbance to each element	32
Figure 8 The Antenna Array Simulator can display the 3D plot of the power radiation beam shape.....	34
Figure 9 The beam pattern of a 3-element ULA which has look direction at 50 degree azimuth using conventional beamformer.....	39
Figure 10 Scenario 1: With 3-element array, two well separated signal sources (DOAs = -30, 20 degrees) can be detected by both beamformers (classical: solid line and Capon: dashed line) in condition SNR = 20dB.....	41
Figure 11 Scenario 2: 3-element ULA, 2 signal sources SNR = 20 dB, classical beamformer (solid line) fails to detect two closed sources (DOAs = -30, -10 degrees) while Capon beamformer can (dashed line).	42
Figure 12 Scenario 3: With 9-element array, three signal sources (DOAs = -60, -70, 20 degrees) , SNR = 20dB. Both beamformers (classical: solid line and Capon: dashed line) fail to detect all three sources: The peaks at -60 and -70 degrees fall on top of each other at angle -65 degrees.....	43

Figure 13 Scenario 4: With 20-element array, three signal sources (DOAs = -60, 70, 20 degrees) , SNR = 20dB. Capon beamformer (dashed-dotted line) can detect all three sources while classical can not.44

Figure 14 DOAs estimation by 3 beamforming methods (Conventional, Capon and MUSIC) with 20-element array47

Figure 15 The normal radiation pattern of the adaptive array (wide separation angle).....49

Figure 16 The extra output power required when the separation angle is small50

Figure 17 The beam patterns of a 4-element linear array using zero-forcing beamforming. The DOA (angle of arrival) of the desired user is at 0° (broadside angle) and the interferer is moving from 40° (dash-dot) to 5° (solid). The overshoot of the main lobe is approximately 9 dB.52

Figure 18 The variation of magnitude of the taps of the 4-element array (zeroforcing beamformer) when the desired user DOA is fixed at 0° and the interferer DOA (null position) swings from -60° to $+60^\circ$. (note that the 1st and the 4th tap have the same magnitude and increase tremendously when the separation angle becomes small) ..53

Figure 19 The output power variation with respect to ϕ_2 the phase of the residual signal in the null direction. Null depth are $-\infty$, -20 dB, -10 dB, -5 dB, and -2 dB. The array has 4 elements, one desired user at broadside angle, one interferer at 10 degrees. ...57

Figure 20 (a) The output power surface of the 3-element array with respect to magnitude and phase of the displacement δ . (b) The cross-sectional of the power surface at different values of $|\delta|$. When $|\delta| = 0$, the array has infinite null at the look direction and therefore no optimum phase can be obtained to minimize the output power.61

Figure 21 The flow diagram of the algorithm for designing antenna array weights with minimum output power. (4-element array, one user and two interferers)63

Figure 22 The output power curve versus the null depth for different separation angle of $10^\circ, 15^\circ, 20^\circ$ 64

Figure 23 Two schemes of powering an antenna array: (a) Separate power amplifiers feeding elements (b) Distributed power amplifiers using Butler (or other similar) matrix and inverse matrix. 66

Figure 24 (a) The relative angular positions of desired and cochannel users composes an angular scenario. (b) The PDF of the desired and cochannel user (equiprobable) 66

Figure 25 The CDF of the output power of the 4-element array with different null depths (∞ , -15 dB, -10 dB, and -5 dB) for the case of *one user and one interferer*. 69

Figure 26 The CDF of the output power of the 4-element array with different null depths (∞ , -15 dB, -10dB, and -5dB) for the case of *one user and two interferers*. 70

Figure 27 Relationship between the magnitude of the taps for a 4-element array in the case of one user and one interferers . (a) Array steers a perfect null. (b) When the array steers a null of -10 dB depth. Contours of constant power are shown. 71

Figure 28 Relationship between the magnitude of the taps for a 4-element array in the case of *one user and two interferers*. Contours of constant power are shown. The null depths are *infinity*..... 74

Figure 29 The plot of the joint CDF of the output power, $P(|w_1| < x; |w_2| < y)$, of the 4-element array in the case of *one user and two interferers*. The null depths are *infinity*. 74

Figure 30 The plot of the joint CDF of the output power, $P(|w_1| < x; |w_2| < y)$, of the 4-element array in the case of *one user and two interferers* with the *null depths ≤ -10 dB*. Antenna performance (utility) is significantly improved. 75

List of Abbreviations

AAS	Antenna Array Simulator
AMPS	Advance Mobile Phone System
AOA	Angle of Arrival
AOD	Angle of Departure
AWGN	Additive White Gaussian Noise
BER	Bit-Error-Rate
BFN	Beamforming Network
BTS	Base Transceiver Station
CCI	Co-channel Interference
CDF	Cumulative Distribution Function
CDMA	Code Division Multiple Access
CMA	Constant Modulus Algorithm
CSI	Channel State Information
DMI	Direct Matrix Inversion
DOA	Direction of Arrival
GSM	Global System for Mobile
GUI	Graphical User Interface
ISI	Inter-Symbol Interference
LMS	Least Mean Square
MAI	Multiple Access Interference
MCM	Multi-user CDMA MIMO
MIMO	Multiple-Input Multiple-Output
ML	Maximum Likelihood
MMSE	Minimum Mean-Squared Error

MUSIC	Multiple Signal Classification
N-RLS	Normalised Recursive Least Square
NDC	Null Depth Control
PA	Power amplifier
PN	Pseudo Noise
RAKE	The rake receiver is a technique which uses several baseband correlators to individually process multipath signal components. The outputs from the different correlators are combined to achieve improved reliability and performance
RLS	Recursive Least Square
SINR	Signal-to-Interference plus Noise Ratio
SNR	Signal-to-Noise Ratio
STD	Space-Time Decorrelator
TDMA	Time Division Multiple Access
UCA	Uniform Circular Array
ULA	Uniform Linear Array
WCDMA	Wideband Code Division Multiple Access
ZF	Zero-Forcing

1 Introduction

Wireless technologies are approaching to the third generation. The rapidly growing demands on wireless communication systems create the need for techniques that increase the system capacity. The adaptive antenna array is a favourite solution for the capacity problem. The exploitation of the new space/angle dimension of the signal in addition to other well known dimensions such as frequency, time or code can help the system transmit less power with more precision. This yields to a reduction of interference and therefore increases the system capacity.

The goal of wireless communications is to provide a wide variety of voice and data services. The transmission of non-voice data streams such as email messages with rich text format, high resolution digital images, video clips or computer data files requires higher and higher bandwidths. This requirement unfortunately consumes the allocated user bandwidth and reduces the system capacity. Moreover, frequency or code reuse schemes may lead to excessive multiple access interference (MAI) or co-channel interference (CCI) [2]. This will limit the number of users that can simultaneously use the same base station and thus leads to reduction the overall system capacity.

The use of adaptive antenna arrays at the base station will significantly reduce MAI. The use of optimum combining techniques using spatial diversity provided by the antenna array will also mitigate the multipath fading effect. The use of adaptive beamforming at the base station (BTS) will significantly improve performance of the transceiver in both uplink and down link. In the uplink: the base station with adaptive antenna array will have more immunization to interference by steering the main beam and nulls towards the desired user and MAI sources. In the downlink: the adaptive array can concentrate the

transmit power to a relatively narrow spatial angle toward the desired user (because the direction of the desired user has been detected before through uplink channel estimation) and therefore reduce the amount of interference to other mobile users significantly.

2 Motivation and Background

2.1 Motivation

As mentioned above, the application of adaptive antenna arrays in mobile cellular communication systems becomes more popular and realistic at the commercial level. The adaptive antenna array at the base station is used for automatic optimization of the transmitting or receiving pattern in response to signal environment.

The adaptive antenna array has been empowered with a variety of adaptive algorithms. These algorithms are the signal processing strategies to determine the optimum set of antenna element weights in response to signal conditions including the changing of position of mobile stations or multipath-fading scenario. These algorithms fall into two major categories:

- 1- *Reference based adaptive algorithms.*
- 2- *Direction-of-arrival (DOA) based adaptive algorithms*

The reference based adaptive algorithms use knowledge of a desired reference signal together with measurement of the received signal to adaptively change the antenna weights according to a predefined criterion such as maximum signal to interference and noise ratio (SINR)[1][3][5][6][7].

In contrast, the DOA based algorithms use the specific mathematical method to extract the DOA of all mobile users sharing the same frequency band including the DOAs of desired user as well as co-channel interferers and the DOAs of the multipath reflections of these original sources of signals [3][4]. Once the natures of signal sources are determined, the adaptive antenna will form an appropriate beam pattern to boost the desired signal and

suppress the interferences. The optimized beam pattern will have the nulls steered at the interference sources and the main beam steered to the desired user's direction [25].

The performance of the adaptive antenna array is greatly degraded when the separation angle (i.e. the spatial angle between desired user and closest interferer DOAs) is too small. If the separation angle is smaller than a certain threshold the adaptive antenna will fail to form a correct pattern. It would rather form an erroneous pattern that will deteriorate the desired signal reception. The threshold of the separation angle at which the adaptive antenna array still operates effectively is directly proportional to the beamwidth of the antenna array. The beamwidth in turn depends on the number of antenna elements which is associated with the cost of the array. The smaller beamwidth the better array resolution and the higher cost of the system.

This thesis proposes a flexible technique to alleviate this shortcoming of the adaptive array by reducing effective beamwidth without increasing the number of antenna elements. This technique creates a new optimization criterion for beamforming by trading off the null depth for smaller beamwidth and therefore smaller separation angle. The new beamforming criterion will make the adaptive antenna array operate more efficiently while the separation angle is small. It helps to reduce the transmitting power of the whole array and therefore reduce unwanted spectrum pollution in the transmitting process. The new beamforming criterion can also help reduce the background noise for the received signal by not boosting the gain of the antenna pattern in the unwanted direction when the base station is working in the receiver mode and while the separation angle is small.

2.2 Problem statement

Adaptive antenna arrays have been used to form a time-varying beam pattern by steering nulls toward the interference sources (jammers) to suppress the interference while keeping a unit response at the direction of the desired user. The beamforming capability of the adaptive antenna array can be assessed by its accuracy and flexibility. Ideally, the perfect “smart” antenna can steer the main beam and nulls to any random directions within the range of -90^0 to $+90^0$. Naturally, when the positions of null and peak are too close, the array with a limited number of elements cannot form such a beam pattern. In order to form such kind of beam, it is required to have an array with infinite number of elements. This is just an unrealistic idea [25]. Antenna array radiation patterns are not spiky shaped, but consist of lobes with notches (nulls) in between. Figure 1 and 2 shows the radiation pattern of a uniform linear array with 4 and 9 elements. Thus antenna arrays cannot reject interference sources that are too close to the desired user or “look direction”. The number of lobes and nulls are the same and equal the number of antenna elements minus one.

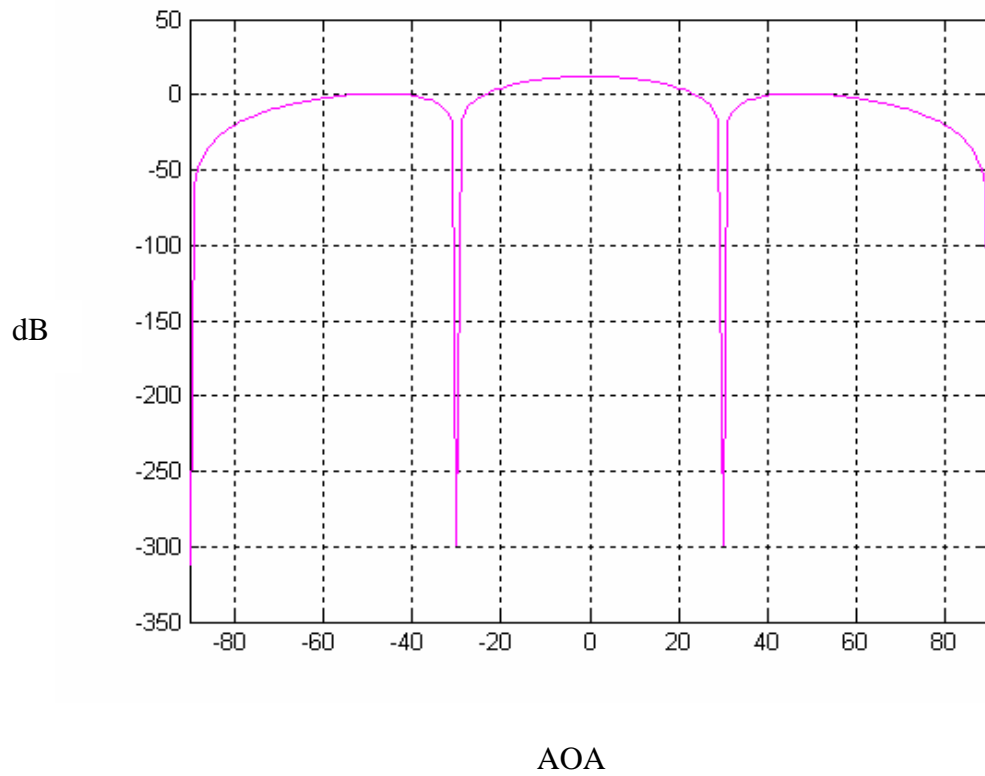


Figure 1 The four- element antenna array radiation pattern (in dB scale)

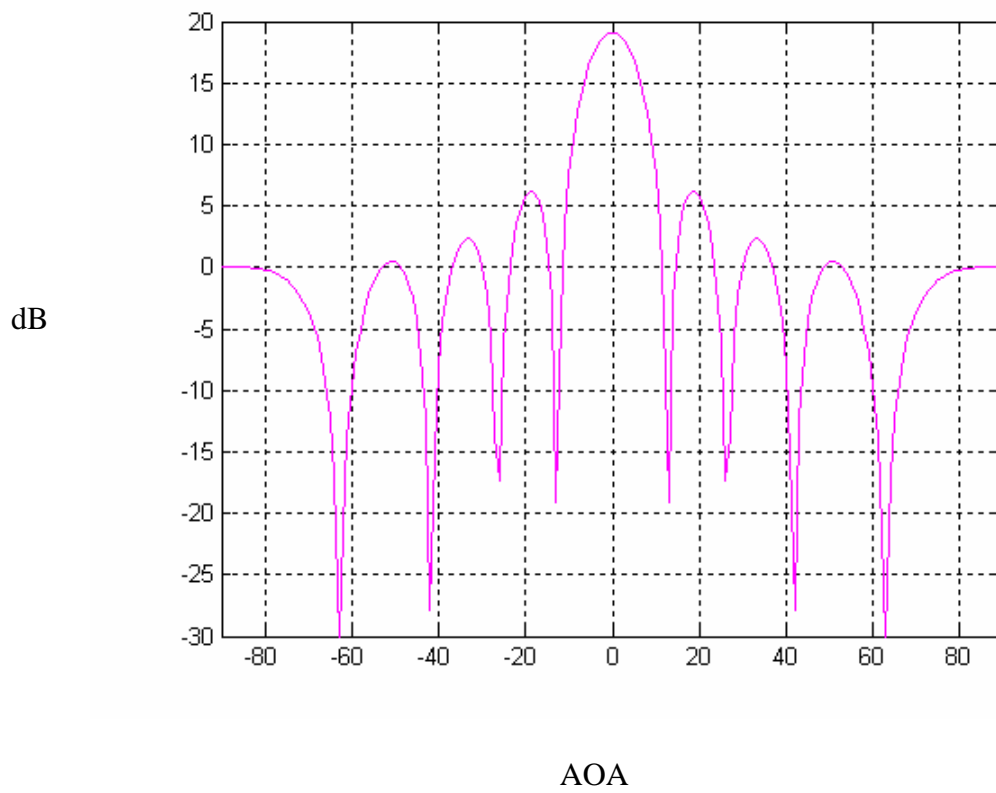


Figure 2 The nine- element antenna array radiation pattern (in dB scale)

These figures clearly show that the minimum beamwidth (i.e. the smallest angular distance between two consecutive nulls of the beam pattern) is inversely proportional to the number of antenna elements. The beamwidth is approximately equal 50° and 20° for the 4 and 9-element array respectively. When the spatial separation (i.e. spatial angle between desired user and interference source) is less than the minimum beamwidth, a handover (channel reallocation) is mandatory due to an unacceptable SINR (signal-to-interference-and-noise-ratio) on the uplink and an increase in downlink transmission power. The compulsory handover (hand off) will decrease the utility of the array and indirectly reduce the system capacity of a cell. This thesis presents a technique that can be used to reduce the separation angle limit between the desired user and the co-channel interferer while keeping CCI from cochannel users below a predefined threshold and without increasing the number of antenna elements. The technique is based on an optimisation process, which trades off the null depth (normally infinity and therefore unnecessary) for reduced transmission power. This technique is essentially reshaping the array beam patterns by reducing the null depths and also reducing the overshoot of the main lobes when the array attempts to steer nulls too close to look direction.

During the investigation, it was discovered that the power distribution among the antenna array elements is greatly non-equal when steering nulls. It implies that the appropriate dimensioning of the power amplifiers feeding each antenna element will lead to a reduction in the cost of the basestation.

2.3 Adaptive Antenna Array Principle

2.3.1 Uniform Linear Array (ULA)

The adaptive antenna array consists of N identical controllable radiating elements. These elements are connected to an *adaptive signal processing unit* (also called the *weight generation unit*). The geometry of the antenna array can vary widely, but the most common configuration is to place the isotropic elements along a straight line with equal inter-element spacing (*uniform linear array*, ULA). In the scope of this thesis, only the ULA will be investigated. The application of the *uniform circular array* (UCA) is mainly in beam switching rather than beamforming therefore not to be considered herein [4] [25]. A generic ULA is shown in Figure 3; which consists of N antenna elements connected to beamforming networks (BFNs). The BFN can vary both amplitude and phases (weights) of the excitation to the antenna elements such that a variety of output radiation patterns can be created. The BFNs are under the control of *adaptive signal processing unit*, which can be pre-programmed with various adaptive algorithms, thus the array beam pattern, null positions can be automatically adjusted in order to reject the co-channel interference and enhance the performance of the system. Normally, one adaptive signal processing unit can control several BFNs. The total antenna array radiation pattern is a superposition of all radiation patterns created by BFNs.

For uplink, employing TDMA (Time Division Multiple Access) schemes, the base station deals with one desired user at a given time slot. The uplink channel is contaminated with a variety of co-channel signals, multipath copies of the desired signal and noise. The adaptive antenna array detects the desired signal from the noisy channel by a beamforming algorithm. Therefore in the uplink processing, only one BFN operates at a given time slot to peak up the desired signal while rejecting the others. In contrast, for the downlink, the base station simultaneously transmits signals to many mobile users and

therefore many BFNs are operating at the same time to mutually minimize the CCI/MAI among these mobile users.

In the case of Code Division Multiple Access (CDMA), all physical channels are operating in the same frequency band simultaneously. At the basestation receiver, channels can be separated by using the orthogonal property of their code structure. Therefore, the basestation will be using multiple BFNs. However, the *DOAs based beamforming* cannot be applied for CDMA because, the number of cochannel users normally exceeds the number of antenna elements [16]. There are many proposed extensions to the beamforming algorithms that are suitable for CDMA or WCDMA [16]. In the scope of this thesis, we will not consider the beamforming methods for any particular air interface standard such as GSM or CDMA, The purpose of this research is limited to general beamforming algorithms based on the assumption that the DOAs of the main user and interference sources are known to the basestation.

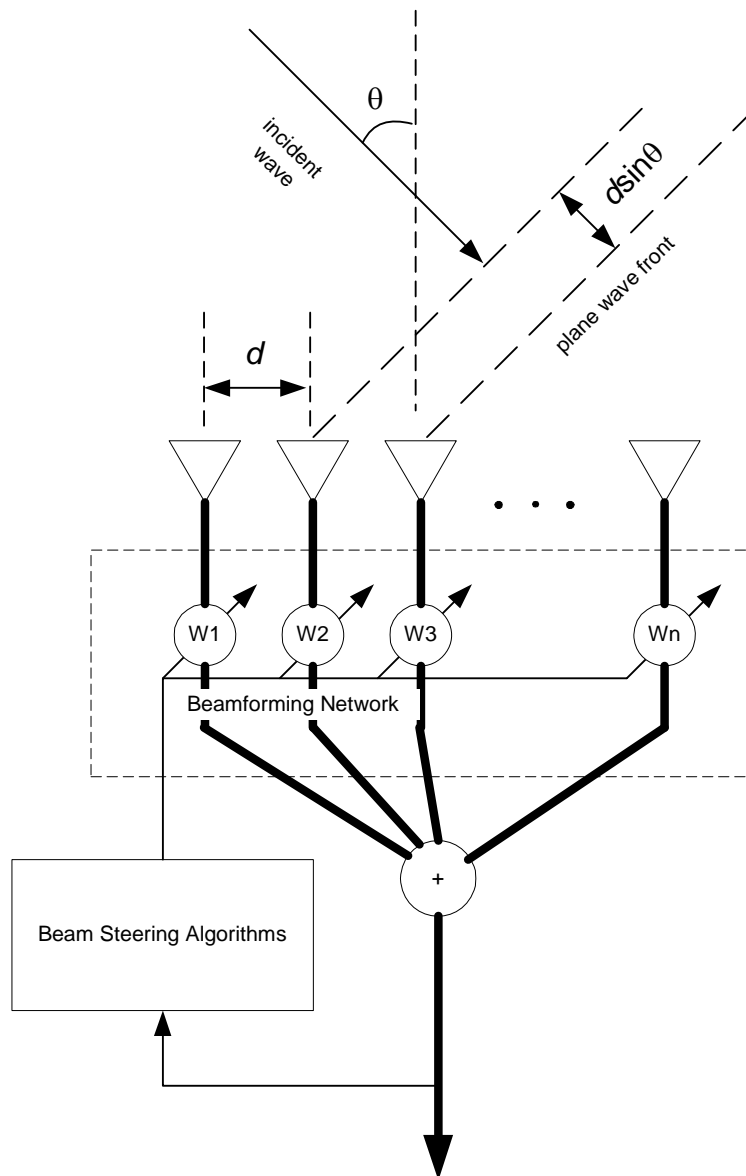


Figure 3 An ULA with plane wave arrives at angle θ

The spacings between the antenna array elements are the same and equal to d . A plane wave arrives at the array from a direction that forms an angle θ to the array broadside direction or the DOA of signal s_1 is θ (figure 3).

The wave front of the incident signal s_1 will arrive to each element of array at different time (in this case, the incident wave arrives at element 1 first and then element 2 and so on). The different time of arrival at each array element will cause a slight phase shift of the received signal at the array outputs. Due to this phase shift the array processor can

determine the DOA of the incident wave by processing the whole array outputs at each sensor. In real life, the complex signal arriving at array sensors is a combination of many signal sources that impinging at different angles and its multipath reflection. This is a very complicated mixed signal environment that can be analyzed by either time or space processing or a combination of both. The RAKE receiver is an example of purely time processing (using one sensor element for many fingers processing). Adaptive antenna array is an example of space-time processing. Many powerful space-time processing techniques exploit the time of arrivals differences and code structures of the signals to separate the desired and unwanted signals from a mixed received signal.

The following is a calculation of the phase shift due to difference in time of arrival of the wave front: Let

$$\tau = \frac{d \sin \theta}{c} \quad (1)$$

be the time of arrival difference at two consecutive array elements,

c is speed of light $c = 3 \times 10^8$ m/s.

If the incident wave has frequency of f (Hz) then angular frequency

$$\omega = 2\pi f = \beta / \tau \quad (2)$$

$$\text{where } \beta \text{ is phase shift, the wave length } \lambda = \frac{c}{f} \quad (3)$$

$$\text{hence } \beta = \omega \tau = \frac{2\pi f d \sin \theta}{c} = \frac{2\pi d \sin \theta}{\lambda} \quad (4)$$

is the phase shift of signal at antenna array output.

For the N-element ULA the phase shift of the signal with respect to the reference element (normally the first element) will be characterized in the array steering vector:

$$a(\theta) = \begin{bmatrix} 1 & e^{j\left[\frac{2\pi d}{\lambda} \sin \theta\right]} & e^{j\left[\frac{4\pi d}{\lambda} \sin \theta\right]} & \dots & e^{j\left[\frac{2\pi d}{\lambda} (N-1) \sin \theta\right]} \end{bmatrix}^T \quad (5)$$

Array steering vectors are the spatial signatures of signals. The array output vector therefore equals the product of the array steering vector and the signal vector.

$$X(t) = [x_1(t) \quad x_2(t) \quad \dots \quad x_N(t)]^T = s(t)a(\theta) \quad (6)$$

2.3.2 Uplink and Downlink Channel Model

Mobile cellular communication systems have two radio links: the uplink from mobile to the base station (also known as the reverse link) and the downlink from the base to the mobile (also known as the forward link).

2.3.2.1 Uplink

Consider a cell site with an array of N antennas. The number of mobiles in use is L , that is equivalent to L signal sources s_1, s_2, \dots, s_L composing the signal vector

$$S(t) = [s_1(t) \quad s_2(t) \quad \dots \quad s_L(t)]^T \quad (7)$$

where $[\cdot]^T$ denotes the transpose operator.

The spatial positions (i.e. DOAs) of those mobile units are $\theta_1, \theta_2, \dots, \theta_L$ defining multiple steering vectors $a(\theta_i) \quad i=1,2,\dots,L$. The steering vector takes the form:

$$a(\theta_i) = \begin{bmatrix} 1 & e^{\frac{j2\pi d}{\lambda} \sin \theta_i} & \dots & e^{\frac{j2\pi d}{\lambda} (N-1) \sin \theta_i} \end{bmatrix}^T \quad (8)$$

All of these steering vectors are combined in one matrix so called the array manifold, which represents the spatial signature of all primary signal sources which have the DOAs $\theta_1, \theta_2, \dots, \theta_L$. The following is the expression for the array manifold:

$$A(\Theta) = [a(\theta_1) \quad a(\theta_2) \quad \dots \quad a(\theta_L)] \quad (9)$$

As shown in Figure 4, each input $x_1(t), x_2(t), \dots, x_N(t)$ from the array receives the combination of all signal source s_1, s_2, \dots, s_L and these array inputs can be expressed in term of a column vector:

$$X(t) = [x_1(t) \quad x_2(t) \quad \dots \quad x_N(t)]^T \quad (10)$$

The array input vector $X(t)$ is the product of array manifold $A(\Theta)$ and signal vector $S(t)$

$$X(t) = A(\Theta)S(t) + N(t) \quad (11)$$

where

$$N(t) = [n_1(t) \quad n_2(t) \quad \dots \quad n_N(t)]^T \quad (12)$$

is the additive noise at each element.

The output of the array, $Y(t)$ is a weighted combination of N inputs $x_n(t) \quad n=1,2,\dots,N$ as follows:

$$Y(t) = W^H X(t) \quad (13)$$

where

$$W = [w_1 \quad w_2 \quad \dots \quad w_N]^T \quad (14)$$

is the weight vector of the antenna array. This weight vector is updated according to the change in the signal environment caused by movement of all mobile users. $[\cdot]^H$ denotes the Hermitian transpose operator.

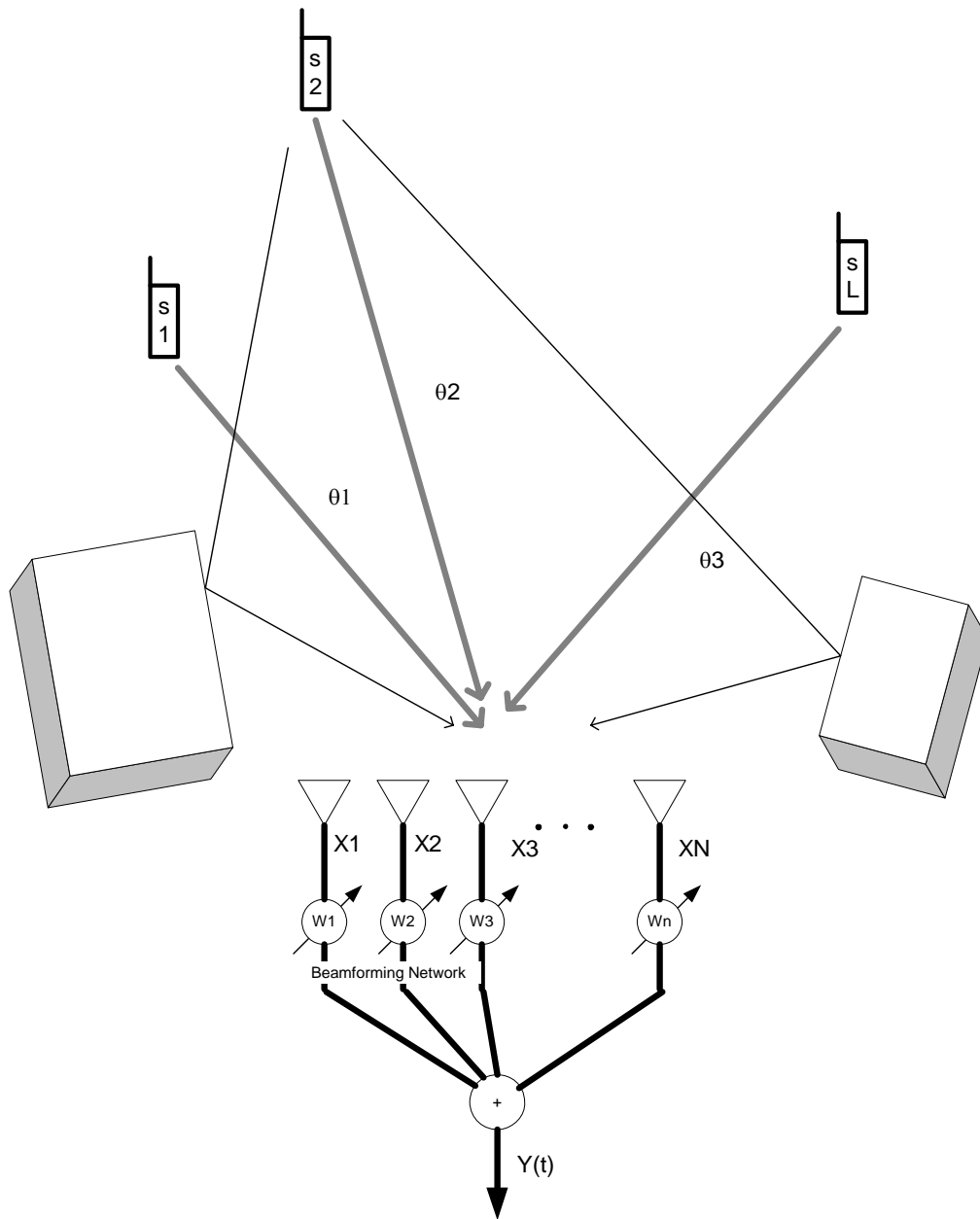


Figure 4 Uplink: the base station receives signals and multipath copies from mobiles.

2.3.2.2 Downlink

The mobile users now receiving the base-station signal via downlink frequency f_D . The base-station transmits signals $s_{d1}, s_{d2}, \dots, s_{dL}$ to the corresponding L co-channel users r_1, r_2, \dots, r_L . In this case, the basestation uses L beamforming networks to form L independent radiation patterns that maximize the transmit power to corresponding user. Each of the beamformer consists of N weight elements :

$$W_i = [w_i^1 \quad w_i^2 \quad \dots \quad w_i^N]^T \quad (15)$$

where $1 \leq i \leq L$ is the index of beamformer.

The composite signal at the tip of the antenna elements $X(t)$

$$X(t) = W^H S(t) = \begin{bmatrix} W_1 & W_2 & \dots & W_L \end{bmatrix} \begin{bmatrix} s_1(t) \\ s_2(t) \\ \dots \\ s_L(t) \end{bmatrix} = \begin{bmatrix} X_1(t) \\ X_2(t) \\ \dots \\ X_N(t) \end{bmatrix} \quad (16)$$

where W is a matrix of downlink weighting vectors. Each of these vectors, $W_i, i=1, \dots, L$, corresponds to the one radiation pattern for each user. In other words, the adaptive antenna array at the basestation has L beamforming networks working in parallel to form L distinctive beam patterns with L different “look directions”.

The received signal at the K -th mobile user is a product of the composite signal $X(t)$ with the steering vector $a(\theta_K)$

$$R_K(t) = a(\theta_K) W^H S(t) + N(t) \quad (17)$$

The weight vectors W_i can be derived from the uplink DOA estimation process. Basically, the downlink weight vectors must be designed so that ideally, the K -th mobile user only receives signal S_K and none of the other signals S_i where $i \neq K$.

In other words, the weight vectors W_K

$$W_K = [w_K^1 \quad w_K^2 \quad \dots \quad w_K^N]^T$$

must form a radiation pattern that has a main lobe steered towards the K -th mobile user and nulls towards all other users. The major problem of designing downlink beamforming is channel estimation, because the basestation normally has no feedback from mobile users to update the channel information [23]. In the scope of this thesis we propose a simple low cost downlink beamforming method that only uses the DOAs estimated in the Uplink array processing to design the beam that mutually cancels MAI among users. This is a *zero-forcing algorithm* and it will be investigated in the following sections

The downlink beamforming effectively concentrates the transmitted energy in the direction of the desired user and thus reduces the disturbance to the mobile users operating in the other cells with the same downlink frequency. Note that in this case L_u , the number of mobile users maintaining the radio link with the base station is not the same as the L , the number of signal sources including interference and multipath in the uplink case mentioned above. The number of users served by the base station should be much less than the number of signal sources mentioned above in uplink case.

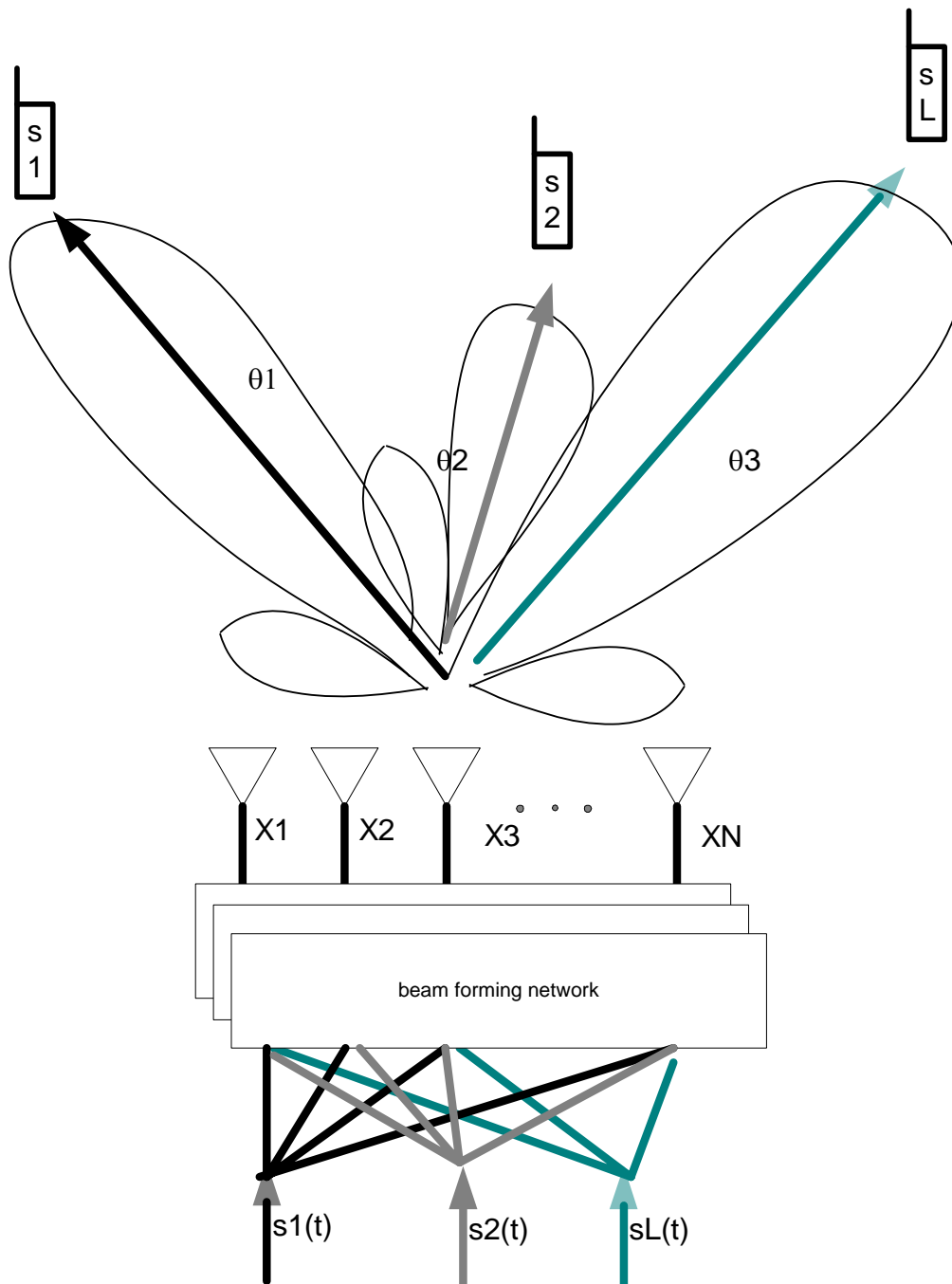


Figure 5 Downlink: the base station transmits signals to co-channel users.

2.4 Antenna array simulator

2.4.1 Study of the variation of the antenna array beam patterns

The antenna array radiation pattern is a function of a number of factors such as: the number of elements, the inter-element spacing, the magnitude and the phase of sensor weights, polarisations of the sensors and sensor radiation pattern. The variation of each factor will change the shape of the array beam pattern dramatically. The Antenna Array Simulator visualises the effects of changing of these factors. The visualisation helps the array designer to have more understanding about antenna arrays without building a costly array prototype. In the scope of this thesis, we can assume that array consist of all identical ideal point source elements.

2.4.2 Basic antenna array simulator

The *basic antenna array simulator* was created in order to explore uniform linear array (ULA) and uniform circular array (UCA) radiation pattern as functions of the following factors:

- Array geometry: linear, circular, planar array...etc.
- Array symmetry: inter element spacing, magnitude, and phase of the element.
- Array uncertainties: spacing errors, magnitude and phase errors.
- Array response to signal environment: beam pattern changing according to changes of the signal environment.

The *basic simulator* allows us to obtain simulated radiation patterns of an array while selecting the following parameters:

- The array shape L or C : linear or circular.
- The number of elements N : from one up to twenty elements.
- The inter-element spacing d : any factor of a wavelength λ (normally $d = \lambda/2$).

- The variation of complex element weights W_i : uniform, non-uniform. The individual tap weight can be entered manually or imported.
- The imported weight vectors, which are results of an adaptation process: The weight vectors can be imported sequentially to show the progress in an adaptation process.
- The variation of the desired user's DOA or interferers' DOAs: The signal conditions can be varied to invoke the adaptation process and updating the tap weights.

The basic antenna array simulator will give the traces and statistics of the following things:

- The radiation pattern: number of lobes, nulls and its position as well as attenuations.
- The total output power: can be plotted as a spatial power spectrum.
- The variation of the tap weight (magnitude and phase) as a function of desired user's DOA or interferers' DOAs.
- The mean squared error of the array output comparing with reference signal in the adaptation process.

The results of the *basic antenna array simulator* can be used for study the effect of phased array response to changes in the major array factors. These changes reflect in changes in radiation patterns such as beamwidth, maximum side lobe, grating lobe...etc. The basic simulator can also be used to sequentially simulate the variation of one factor such as inter-element spacing or phase of the tap weight. The graph will display the radiation pattern according to the prescribed variation (as shown in figure 6).

Figure 6 shows the graphic user interface of *basic antenna array simulator*.

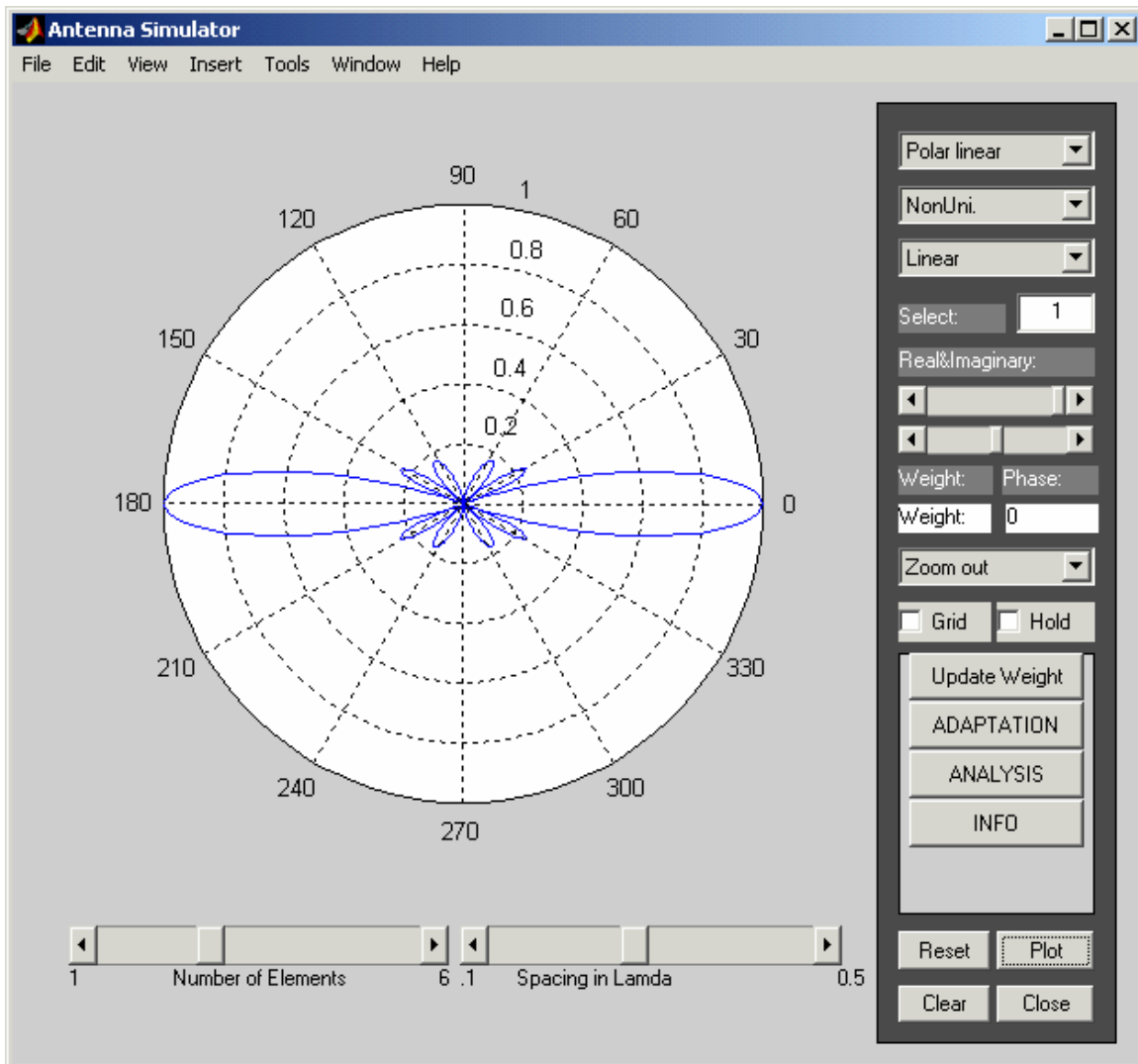


Figure 6 Basic Antenna Array Simulator GUI

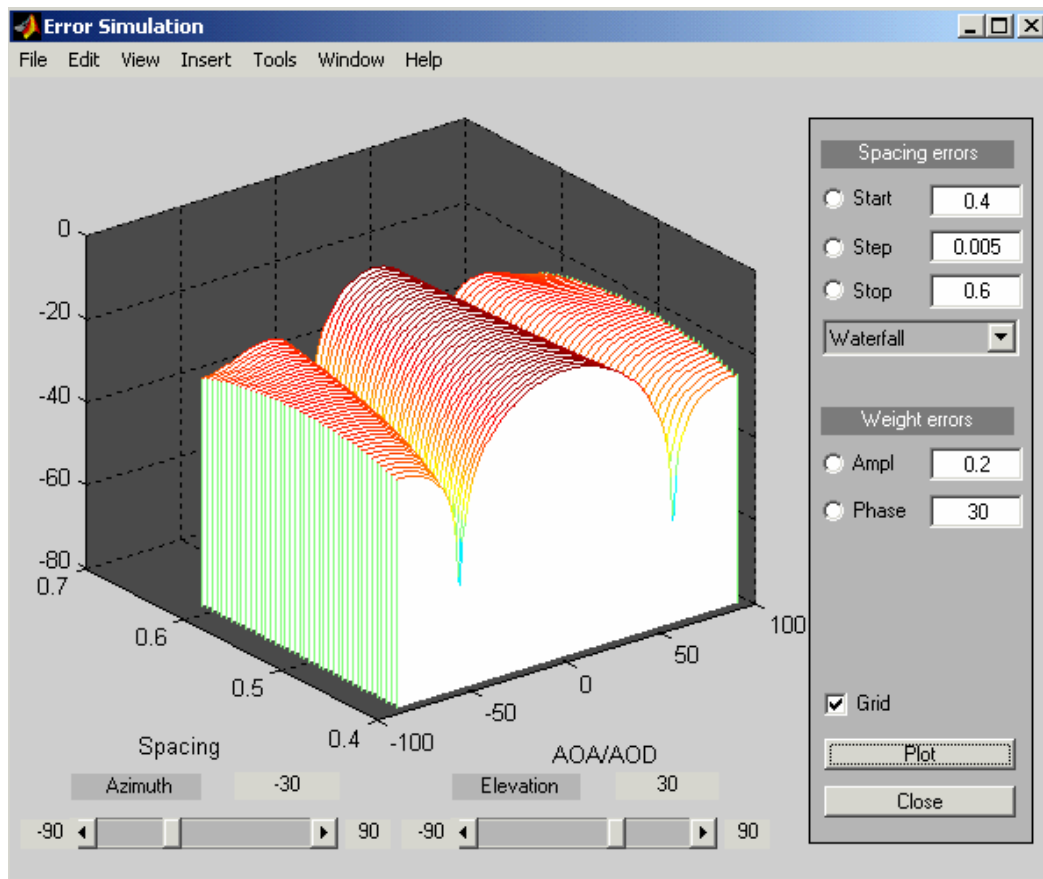


Figure 7 By changing a few factors, the antenna simulator can display the variation of the radiation pattern. This feature can be used to predict behaviour of the array under effect of error or disturbance to each element

The main features of basic antenna array simulator are:

2.4.3 Plotting antenna array radiation pattern

The complex array response at angle θ can be expressed in the following formula:

$$G(\theta) = W^H a(\theta) \quad (18)$$

where W is weight vector and $a(\theta)$ is array steering vector. Equation (18) can be expanded as:

$$G(\theta) = \begin{bmatrix} w^*_1 & w^*_2 & \dots & w^*_N \end{bmatrix} \begin{bmatrix} 1 \\ e^{\frac{j2\pi d}{\lambda} \sin \theta} \\ \dots \\ e^{\frac{j2\pi d}{\lambda} (N-1) \sin \theta} \end{bmatrix} \quad (19)$$

the absolute value of $G(\theta)$ will be plotted according to the variation of angle of arrival and other factors such as inter-element spacing. In this simulator the inter-element spacing can be selected in term of wavelength λ . The number of elements can be selected by sliding the bar. The mode of display can be selected as polar plot or Cartesian plot.

The scale can be chosen linear or logarithmic. The configuration can be selected between linear array or circular and the non-uniform configuration gives flexibility to select an array with non-uniform inter-element spacing. Clicking on plot button after selecting all the parameters will display the array radiation pattern on the graph area. For more advanced feature of the simulator the buttons ADAPTATION or ANALYSIS can be clicked.

2.4.4 Analysis the error effect by antenna simulator

The physical configuration of the antenna array has tremendous affect on its radiation pattern. The tiny change in physical position or magnitude imbalance between the tap weights may lead to huge distortion or pointing error in beam steering and null steering. For this reason, the antenna array simulator is designed to simulate the error effect of the antenna array. This leads to a saving of time and effort either in mathematical analysis and/or in hardware prototype development. In the scope this thesis the following error effect will be analysed:

- Spacing error: when the ANALYSIS button is clicked the new GUI window will pop up (Figure 14). By setting the error range (e.g. from 0.001λ to 0.1λ with a step of 0.01λ), the waterfall plot gives the entire simulated radiation patterns

mutated from minimum error to maximum error. This gives an idea of the effects caused by random spacing error such as reduced null depth, grating lobes...etc. The errors $\Delta s_1, \Delta s_2, \dots, \Delta s_N$ will be reflected in the final modification of the array response formula as follows:

$$G_E(\theta, d) = \sum_{n=1}^N w_n^* e^{j \frac{2\pi(d+\Delta s_n)}{\lambda} (n-1) \sin \theta} \quad (20)$$

- Magnitude and phase error: The random errors (uncertainties) of magnitude and phase of the complex tap weights can be simulated. First, select the non-uniform mode from main GUI window, click the update weight button to import the latest pre-calculated weight. Go to ANALYSIS in the GUI window and edit the range and the steps of phase or magnitude errors to be simulated. The ZOOM feature can be used to magnify the tiny distortion cause by phase or magnitude error.

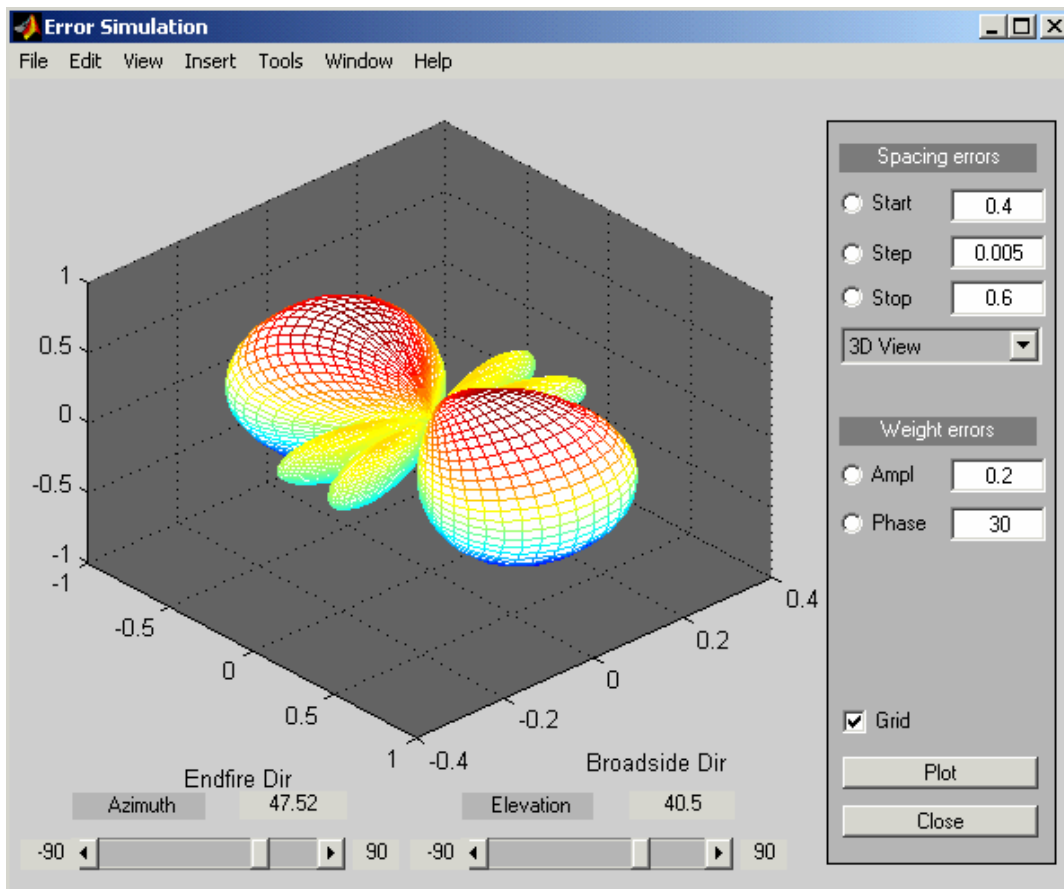


Figure 8 The Antenna Array Simulator can display the 3D plot of the power radiation beam shape

2.4.5 Simulation of adaptation process

This is the most sophisticated feature of the antenna simulator. The purpose of this simulator is creation of a virtual complex signal environment that should have the desired signal, the CCI sources, the virtual multipath copies of all these signal sources. In order to simulate the fading effect, some fading model such as Rayleigh fading can be used. A number of different adaptive algorithms such as Least Means Square (LMS), Recursive Least Square (RLS), Normalised Recursive Least Square (N-RLS), and Direct Matrix Inversion (DMI) are presented here. The simulation results will be returned in terms of the error statistics or output signal to noise ratio with a constellation plot of the output signal after adaptation. However this advanced feature of the antenna array simulator is under development and will be available in the near future.

The *advanced antenna array simulator* can be used to obtain a simulation of the adaptation process. The *advanced simulator* will have channel fading simulator, virtual cellular scenario with mobile users and interference sources simultaneously transmitting signals including multipath reflection. The complex virtual signal environment can be used to verify the operation of the adaptive algorithms and the power distributions among the taps. This will be very useful for the antenna manufacturer to identify the optimum algorithms and optimum configurations without spending on expensive hardware prototyping or creation of a complex signal environment.

The idea of a novel beamforming algorithm was initiated thanks to these preliminary simulations on this simulator. In the next chapter, the novel beamforming criteria will be analysed in depth in mathematical derivation as well as by simulation result. This will be the main part of this thesis.

2.5 Adaptive Beamforming Algorithms

2.5.1 Survey of previous work

An adaptive beamforming network is a device that is able to separate signals collocated in the frequency band but separated in the spatial domain. This provides a means for separating the desired signal from interfering signals. An adaptive beamformer is able to automatically optimize the array pattern by adjusting the elemental control weights until a prescribed objective function is satisfied.

Traditionally, adaptive beamforming has been employed in sonar and radar systems. It started with the invention of the intermediate frequency side lobe canceller in 1959 by Howells [6]. The concept of a fully adaptive array was developed in 1965 by Applebaum [7]. He derived the algorithm that is based on the general problem of maximization of SNR at the array output. Another independent approach to adaptivity uses the least mean square (LMS) error criterion, which was invented by Widrow and Hoff [8]. The LMS algorithm was further developed with the introduction of constraints by Frost [9]. The constraints are used to ensure that the desired signals are not filtered out along with the unwanted signals. Although Applebaum's maximum SNR algorithm and Widrow's LMS algorithm were discovered independently, they are basically similar. For stationary signals both algorithms converge to the optimum Wiener solution [10].

A different technique for solving the adaptive beamforming problem was proposed in 1969 by Capon [11]. His algorithm leads to an adaptive beamformer with a minimum-variance distortionless response (MVDR). In 1974, Reed and his coworkers showed that fast adaptivity can be achieved by using the sample-matrix inversion (SMI) technique [12]. Using this technique, the adaptive weights can be computed directly. Unlike the maximum SNR algorithm and LMS algorithm, which may suffer from slow convergence.

In this proposal, we focus on the downlink beamforming techniques and their associated problems.

2.5.2 Beamforming techniques

Beamforming is essentially a determination of the antenna tap weights to satisfy certain optimum criterion or constraint. Some examples of the optimum criteria are: Maximizing the output power in the look direction θ (*conventional beamforming*) [3], minimizing the noise and interference come from all directions other than θ (*Capon beamforming*) [4], or maintaining unit gain in the look direction θ_0 while zero gain in the interfering directions $\theta_1, \theta_2, \dots, \theta_k$. (*zeros-forcing beamformer*). Different beamforming approaches correspond to different choices of the weighting vector W [4].

2.5.2.1 Conventional beamformer

The conventional (or Barlett) beamformer is a natural extension of classical Fourier spectral analysis to sensor array data [3][13]. This beamformer maximizes output power for a given input signal. Given a signal emanating from direction θ , a measurement of the array output is corrupted by additive noise and written as

$$X(t) = a(\theta)s(t) + n(t)$$

The problem of maximize the output power is formulated as

$$\begin{aligned} \max_W E\{W^H X(t)X^H(t)W\} &= \max_W W^H E\{X(t)X^H(t)\}W \\ &= \max_W \left\{ E|s(t)|^2 |W^H a(\theta)|^2 + \sigma^2 |W|^2 \right\} \end{aligned} \quad (21)$$

The resulting solution is then (see [4])

$$W_{BF} = \frac{a(\theta)}{\sqrt{a^H(\theta)a(\theta)}} \quad (22)$$

The power spectrum can be obtained

$$P_{BF} = \frac{a^H(\theta)\hat{R}a(\theta)}{a^H(\theta)a(\theta)} \quad (23)$$

where \hat{R} is sample covariance matrix and defined by

$$\hat{R} = \frac{1}{M} \sum_{t=1}^M X(t)X^H(t) \quad (24)$$

Figure 9 shows the main beam DOA at $\theta = 50$ degree. The disadvantage of this beamformer is low resolution: any two signal sources that have separation angles smaller than the standard beamwidth of the ULA of $\phi = 2\pi/N$, can not be solved.

The array response is steered by forming a linear combination of sensor outputs

$$y(t) = \sum_{n=1}^N w_n^* x_n(t) = W^H X(t) \quad (25)$$

Given samples $y(1), y(2), \dots, y(M)$, the output power measured by (21)

$$P(W) = \frac{1}{M} \sum_{t=1}^M |y(t)|^2 = \frac{1}{M} W^H X(t)X^H(t)W = W^H \hat{R}W \quad (26)$$

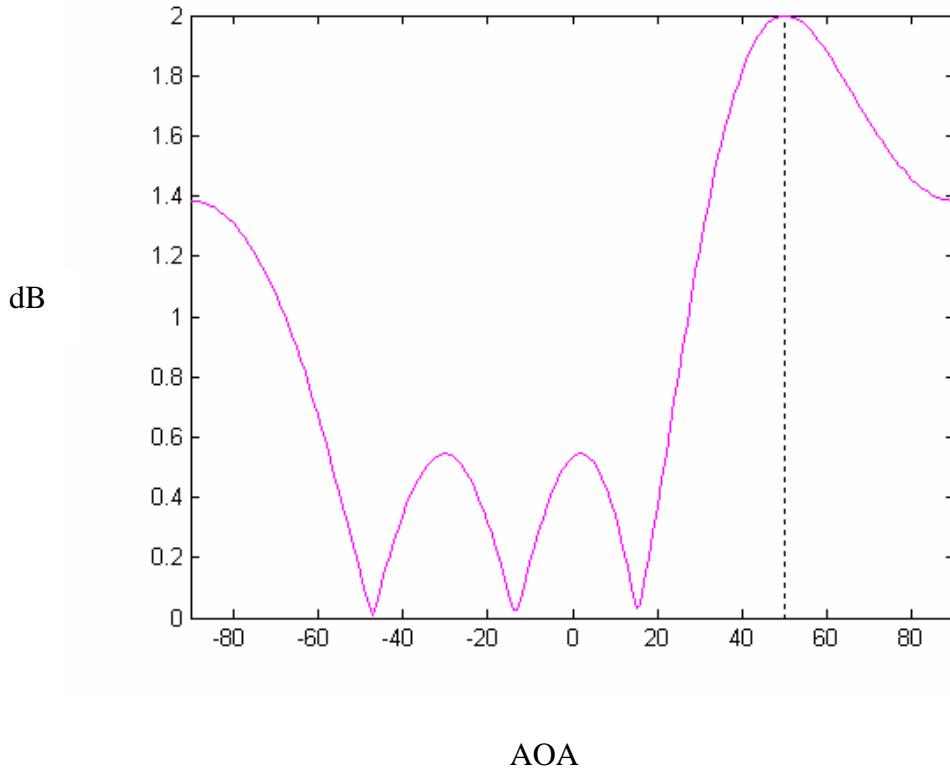


Figure 9 The beam pattern of a 3-element ULA which has look direction at 50 degree azimuth using conventional beamformer.

2.5.2.2 Capon beamformer

The Capon beamformer can resolve separation angles smaller than the beamwidth by modifying the conventional beamforming technique [3]. The optimisation problem was posed as

$$\min_w P(W) \text{ subject to } W^H a(\theta) = 1 \quad (27)$$

where $P(W)$ is the measured output power defined in (21). Hence the Capon beamformer attempts to minimize the power contributed by noise and any signal coming from direction other than θ , while maintaining a fixed gain in the “look direction” θ . The optimal weight can be found by using the Lagrange multiplier technique, resulting in

$$W_{CAP} = \frac{\hat{R}^{-1}a(\theta)}{a^H(\theta)\hat{R}^{-1}a(\theta)} \quad (28)$$

the spatial power spectrum can be obtained as

$$P_{CAP} = \frac{1}{a^H(\theta)\hat{R}^{-1}a(\theta)} \quad (29)$$

It is easy to see why Capon's beamformer outperforms the classical beamformer as given in (20), as the former uses every available degree of freedom to concentrate the received energy along one direction, namely the "look direction". As reflected in (24), the power minimization can be interpreted as sacrificing some noise suppression capability for more focused "nulling" in the direction where there are other interference sources present. The spectral leakage from closely spaced sources is therefore reduced, though the resolution capability of the Capon beamformer is still dependent upon the array aperture and clearly on the SNR [3][4][13].

The comparison of conventional and Capon beamforming method suggests that the optimal weight can be designed to satisfy any specific target criteria (or cost function). This is the motivation for this research. Here, we will investigate the Zero-forcing algorithm [9] and improve it for mobile communications scenarios.

2.5.3 DOA estimation algorithms

The signal sources direction of arrival can be detected by using beamforming technique. The idea is to "steer" the main beam in one direction at a time and measure the output power. The steering location which results in maximum power yields the DOA estimates. The spatial power spectrum can be used to detect the DOAs of all signal sources. In this section we consider a few scenarios with a variety of signal environments and array configurations. This experiment will show the performance of DOA detection methods

based on the above mentioned beamformers. Table 1 summarize the experimental scenarios

Scenario	Number of elements of ULA	Number of signal sources	DOAs (degree)	Separation angles (degree)	Performance comparison	
					Classic	Capon
1	3	2	-30, 20	50	Good	Very good
2	3	2	-30, -10	20	Bad	Good
3	9	3	-60, -70, 20	10, 50	Bad	Bad
4	20	3	-60, -70, 20	10, 50	Bad	Good

Table 1 Performance comparison between Classical and Capon beamformers

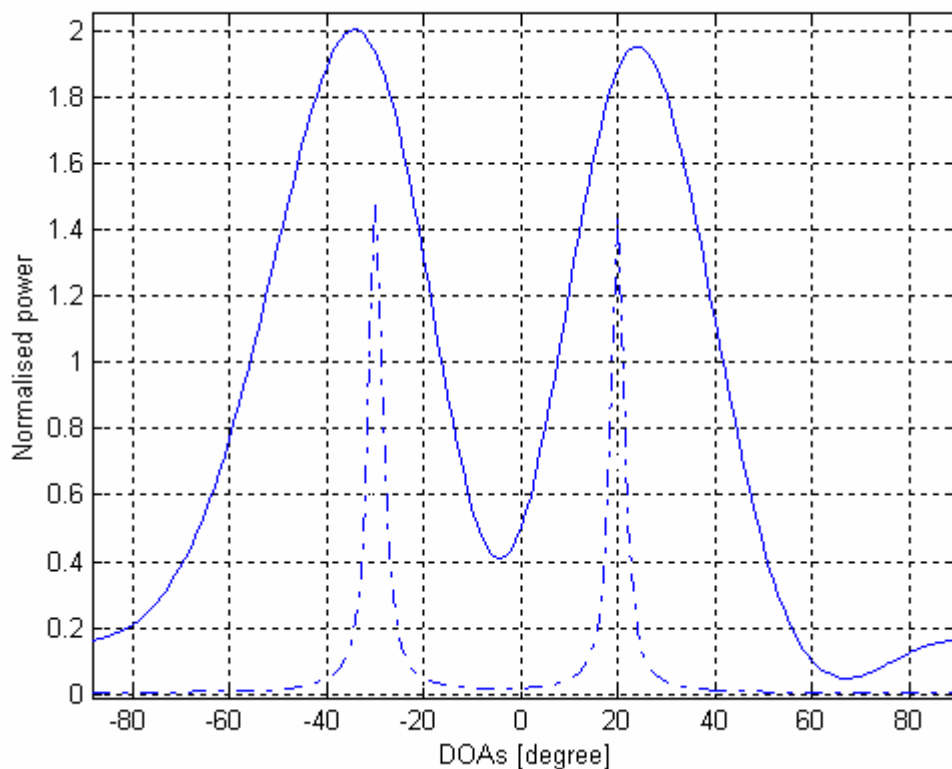


Figure 10 Scenario 1: With 3-element array, two well separated signal sources (DOAs = -30, 20 degrees) can be detected by both beamformers (classical: solid line and Capon: dashed line) in condition SNR = 20dB

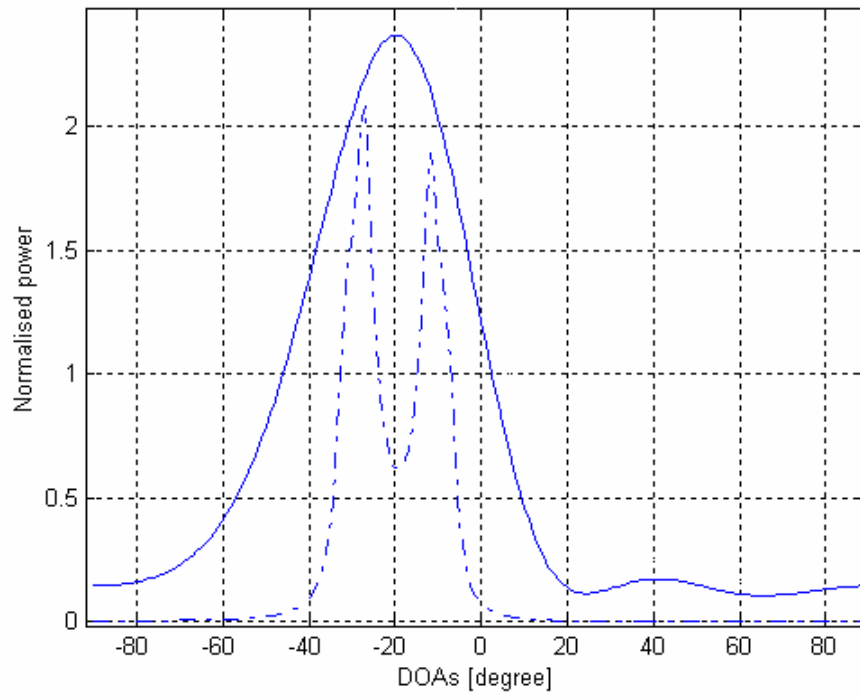


Figure 11 Scenario 2: 3-element ULA, 2 signal sources SNR = 20 dB, classical beamformer (solid line) fails to detect two closed sources (DOAs = -30, -10 degrees) while Capon beamformer can (dashed line).

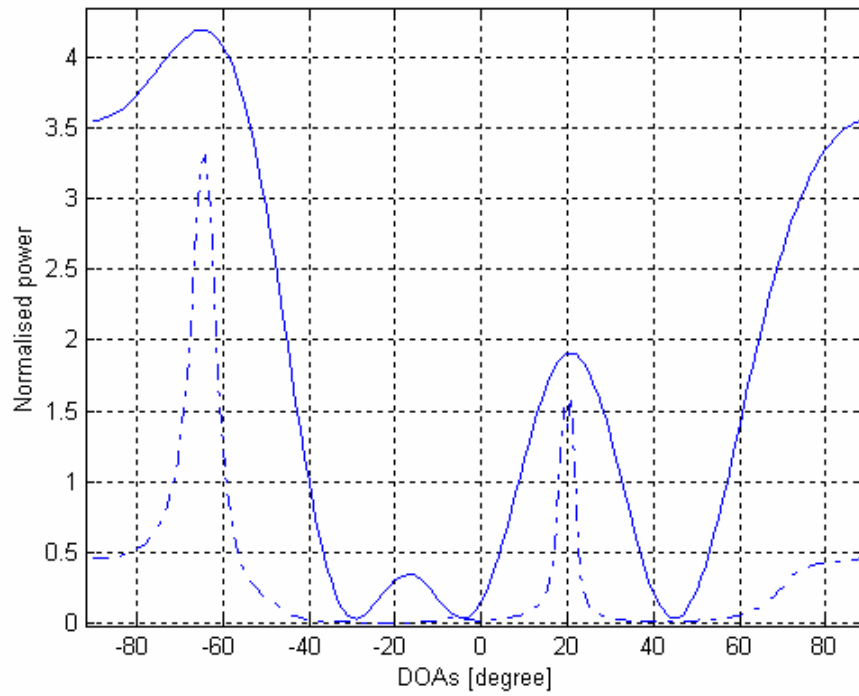


Figure 12 Scenario 3: With 9-element array, three signal sources (DOAs = -60, -70, 20 degrees) , SNR = 20dB. Both beamformers (classical: solid line and Capon: dashed line) fail to detect all three sources: The peaks at -60 and -70 degrees fall on top of each other at angle -65 degrees.

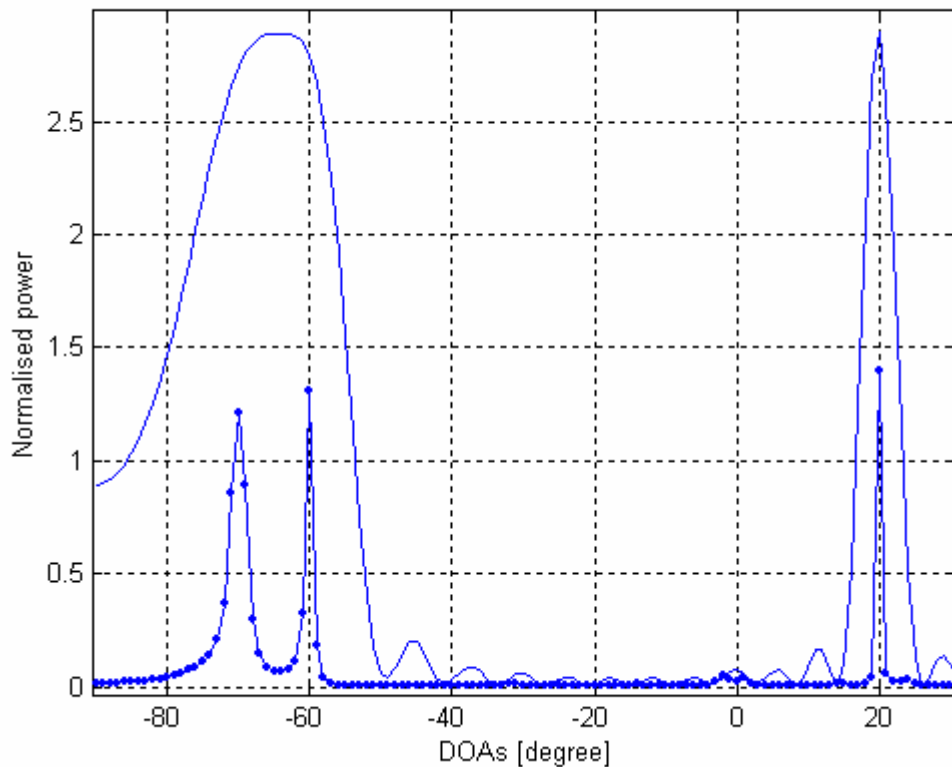


Figure 13 Scenario 4: With 20-element array, three signal sources (DOAs = -60, 70, 20 degrees) , SNR = 20dB. Capon beamformer (dashed-dotted line) can detect all three sources while classical can not.

2.5.4 The MUSIC Algorithm

Many DOA estimation methods in the past, have implicitly called upon the spectral decomposition of a covariance matrix to carry out the analysis [3][4]. One of the most significant contributions came about when the eigen-structure of the covariance matrix was explicitly invoked, and its intrinsic properties were directly used to provide a solution to an underlying estimation problem for a given observed process. The MUSIC (Multiple Signal Classification) algorithm uses the estimated covariance matrix decomposition to separate the signal subspace and noise subspace. These spaces are mutually orthogonal, the spatial spectrum can therefore be obtained by projection on to the noise subspace. The estimated DOAs will appear as the peaks in this spatial spectrum.

Note that the MUSIC algorithm outperforms the earlier mentioned beamforming method such as classical and Capon.

2.5.4.1 Covariance matrix decomposition

The signals arriving at the array are of spatial nature, and thus require the cross-covariance information among the various sensors, i.e. the spatial covariance matrix:

$$R = E\{X(t)X^H(t)\} = AE\{S(t)S^H(t)\}A^H + E\{n(t)n^H(t)\} \quad (30)$$

where $E\{\cdot\}$ denotes statistical expectation,

$$E\{S(t)S^H(t)\} = P \quad (31)$$

is the sources covariance matrix and

$$E\{n(t)n^H(t)\} = \sigma^2 I \quad (32)$$

is noise covariance matrix. The latter covariance matrix is a reflection of the noise having a common variance σ^2 at all sensors and being uncorrelated among all elements.

The covariance matrix R can be expressed as,

$$R = APA^H + \sigma^2 I = U\Lambda U^H \quad (33)$$

with U unitary and $\Lambda = \text{diag}\{\lambda_1, \lambda_2, \dots, \lambda_N\}$ a diagonal matrix of real eigen-values ordered such that $\lambda_1 \geq \lambda_2 \geq \dots \geq \lambda_N \geq 0$. Observe that any vector orthogonal to A is an eigen-

vector of R with the eigen-value σ^2 . There are $N-L$ linearly independent such vectors.

Since the remaining eigen-values are all larger than σ^2 , we can partition the eigen-vectors into noise eigen-vectors and signal eigenvector. Hence, we can rewrite

$$R = U_s \Lambda_s U_s^H + U_n \Lambda_n U_n^H \quad (34)$$

where $\Lambda_n = \sigma^2 I$. Since all noise eigen-vectors are orthogonal to A , the column of U_s must span the range space of A whereas those of U_n span its orthogonal complement. The projection operators onto these signal and noise subspace are defined as

$$\begin{aligned}\Pi &= U_s U_s^H = A(A^H A)^{-1} A^H \\ \Pi^\perp &= U_n U_n^H = I - A(A^H A)^{-1} A^H\end{aligned}\tag{35}$$

therefore:

$$I = \Pi + \Pi^\perp\tag{36}$$

2.5.4.2 The MUSIC algorithm

As noted in previous section (2.3.4.2) the structure of the exact covariance matrix with the spatial white noise assumption implies that its spectral decomposition can be expressed as

$$R = APA^H + \sigma^2 I = U_s \Lambda_s U_s^H + \sigma^2 U_n U_n^H,\tag{37}$$

where, assuming APA^H to be of full rank, the diagonal matrix Λ_s contains L largest eigen-values. $\Lambda_s = \text{diag}\{\lambda_1, \lambda_2, \dots, \lambda_L\}$ a diagonal matrix of real eigen-values ordered such that $\lambda_1 \geq \lambda_2 \geq \dots \geq \lambda_L > \sigma^2$ and $\Lambda_n = \text{diag}\{\lambda_{L+1}, \lambda_{L+2}, \dots, \lambda_N\}$ where $\lambda_{L+1} = \lambda_{L+2} = \dots = \lambda_N = \sigma^2$. To allow for unique DOA estimates, the DOAs must be *unambiguous*, that is the collection of N steering vectors forms a linearly independent set.

In practice, an estimate \hat{R} of the covariance matrix is obtained, and its eigen-vectors are separated into the signal and noise eigen-vectors as in (35). The orthogonal projection onto the noise subspace is estimated as

$$\hat{\Pi}^\perp = \hat{U}_n \hat{U}_n^H\tag{38}$$

and the MUSIC spatial spectrum is defined as

$$P_{MUSIC} = \frac{a^H(\theta)a(\theta)}{a^H(\theta)\hat{\Pi}^\perp a(\theta)}\tag{39}$$

The *estimated spatial spectrum* P_{MUSIC} exhibits the pretty accurate peak at the vicinity of the true DOAs, as shown in the figure 14.

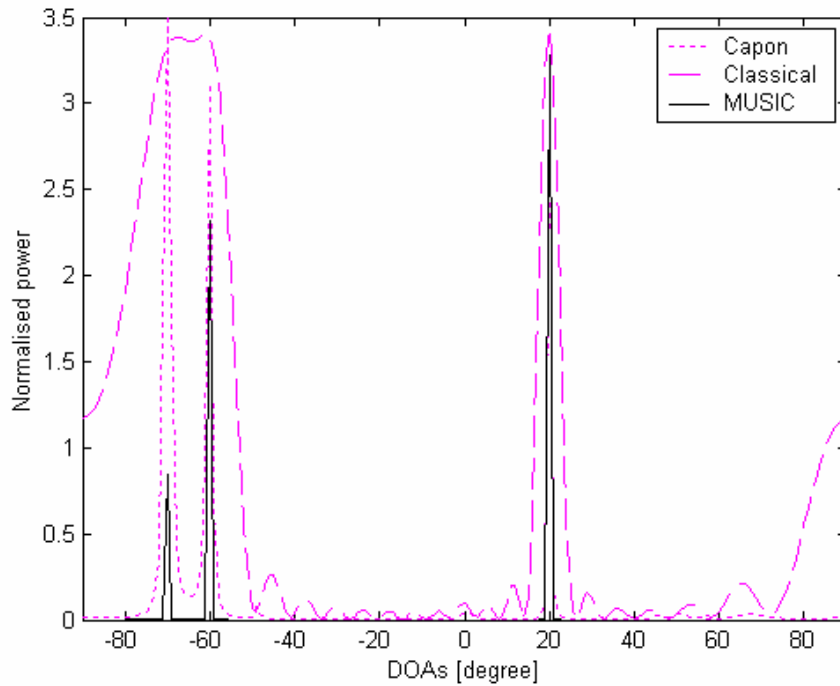


Figure 14 DOAs estimation by 3 beamforming methods (Conventional, Capon and MUSIC) with 20-element array

2.5.5 Selection of downlink adaptive algorithms

Adaptive algorithms are divided into two groups: *reference based* and *DOAs based* algorithms [3]. For the reference-based algorithm, a reference signal (also known as pilot signal) is provided to generate the optimum weights. In the uplink, the reference signal is known to a basestation and therefore it can use the reference-based algorithms (e.g. LMS, RLS or CMA) to form an optimum beam pattern without knowing where the signal comes from. In this case, the basestation has to use the same beam pattern to transmit the signal in the downlink bearing the assumption that the channels are the same for both links. This is not always true and that is why for most of the *reference based* adaptive algorithms, downlink beamforming is not implemented. An alternative option for uplink beamforming is the *DOAs detection method*: The basestation detects the DOAs of the desired and interference signals and forms the beams accordingly: the main beam in the

“look direction” and nulls in the jammers’ directions. In the downlink, the basestation uses the knowledge of the DOAs detected in the uplink processing to generate the beam patterns for each desired users. Among the downlink beamforming algorithms, the *zero-forcing algorithm* is a good candidate, because of its simplicity comparing with the other techniques. Moreover, the zero-forcing algorithm can effectively suppress the jammers as long as the separation angle is large enough. Basically, the zero-forcing algorithm can steer the main beam towards the desired user and form deep nulls towards interferers as long as the system has full knowledge of the directions of the signal sources. The zero-forcing algorithm solves the following simultaneous equations to find the optimum weights, \mathbf{W} :

$$\mathbf{W}^H \mathbf{a}(\theta_0) = 1 \quad (40)$$

$$\mathbf{W}^H \mathbf{a}(\theta_i) = 0; i = 1, 2, \dots, k. \quad (41)$$

Using matrix notation, this becomes:

$$\mathbf{W}^H \mathbf{A}(\Theta) = \mathbf{f} \quad (42)$$

where $\mathbf{A}(\Theta)$ is array manifold and \mathbf{f} is a constraint vector,

$$\mathbf{f} = [1 \quad 0 \quad \dots \quad 0]^T, \quad (43)$$

which imposes a unity gain of the radiation pattern towards the desired user and zero gains towards the interferers. The advantage of the zero-forcing algorithm is that it does not require either reference signal or covariance matrix.

2.5.6 A "difficult" situation for the adaptive array

From the results of investigation, it is revealed that the adaptive antennas for the downlink need to transmit extremely high output power when the signal sources are located at close angles. This unwanted power causes strong interference to other co-frequency cells and increases of the size of the transmitting amplifier at the base station as well as the power consumption. This phenomenon can be referred to as the "difficult" situation for the adaptive array. In such a situation, the adaptive array fails to meet the power constraint requirement and consequently causes clipping in the output amplifier. Developing a technique to mitigate this phenomenon is the motivation of this research. Figure 15 and 16 illustrate this point.

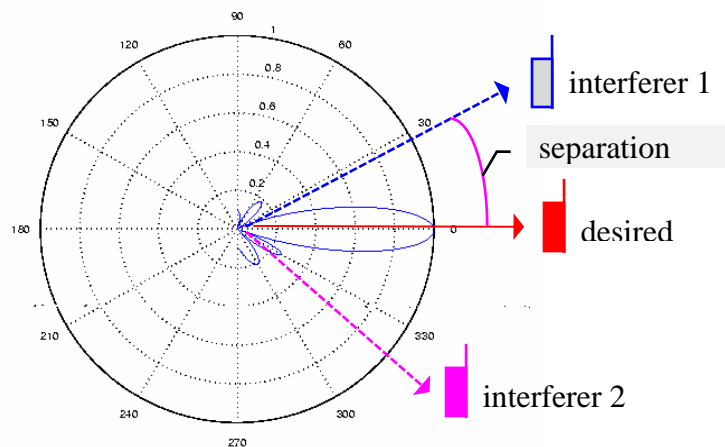


Figure 15 The normal radiation pattern of the adaptive array (wide separation angle)

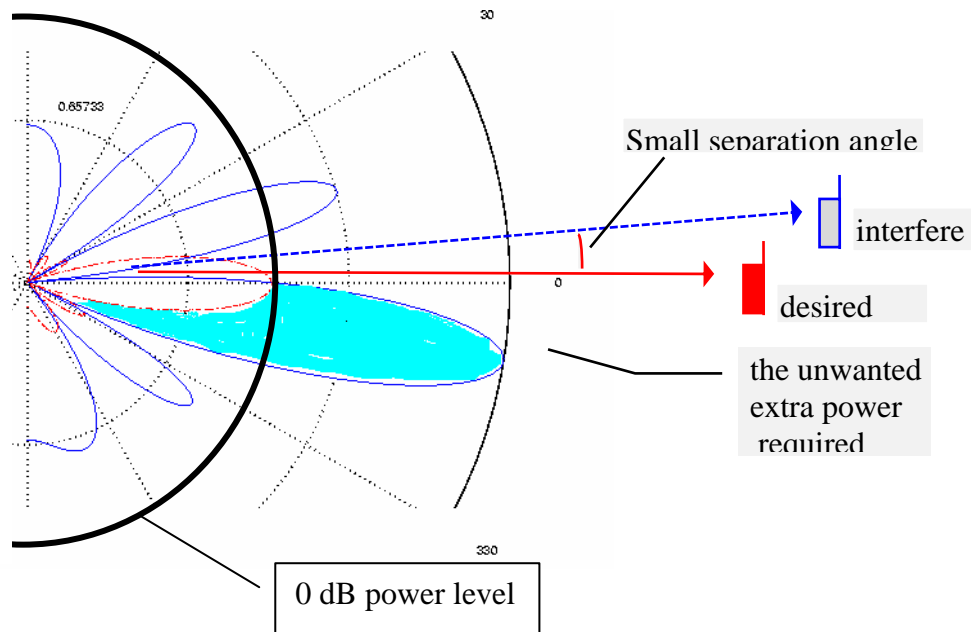


Figure 16 The extra output power required when the separation angle is small

Figure 16 shows the extra output power required when the separation angle is small. The dotted line beam pattern represents the normal case when the user and the interferer are well separated, while the solid beam pattern represents the case when the separation angle is small. The shaded region roughly shows the unwanted extra output power required in order to form a null at 5° (interferer) and a unit gain at 0° (desired user). The extra output power increases exponentially as the interferer approaches the desired user. The rate of increase depends on the number of the elements of the array.

3 Novel beamforming criterion

3.1 *Observation of output power increasing when separation angle is small*

Adaptive antenna arrays at the base station demonstrate crucial advantages over conventional antennas due to their beamforming ability that can effectively focus energy towards the desired user and cancel the interference by null steering. In the radiation pattern, the adaptive array normally puts nulls towards the interferers and the main beam toward the desired user. However, when the null direction is approaching the desired user direction, (e.g. the spatial separation becomes smaller) the resulting beam pattern will have a growth of the main lobe and that causes additional inter-cell interference in the downlink and noise enhancement in the uplink (Figure 17). That situation must be terminated by a compulsory handover. Figure 18 plots the magnitude of the tap weights estimated by a zero-forcing beamformer against the angle of arrival (DOA) of the dominant jammer for a 4-element uniform linear array with a broadside look direction (e.g. the desired user is at broadside angle. The 0 dB line represents the tap power for beamforming without null steering. The transmission power is minimum in this condition and all taps have equal power normalised to $(1/N)^2$ (N is the number of antenna elements). The Figure 17 indicates the increase in transmit power required when null steering is added to beam steering of the main lobe. The overshoot of the main lobe is approximately 9 dB when separation angle is 5 degrees . The magnitude of the all taps increases drastically when the separation angle decreases to zero (Figure 18). The outermost taps are affected mostly and the power required across the array can be quite non-uniform. The total array output power is minimum when the null position is 30° . This is the natural null position for the array and all the tap weights are equal. Any other

position of the null causes an increase in transmission power. This can have implications on the design of the array, particularly the dimensioning of the power amplifiers feeding each antenna. In this chapter we address the problem and propose a method to improve the performance of adaptive arrays in such situations.

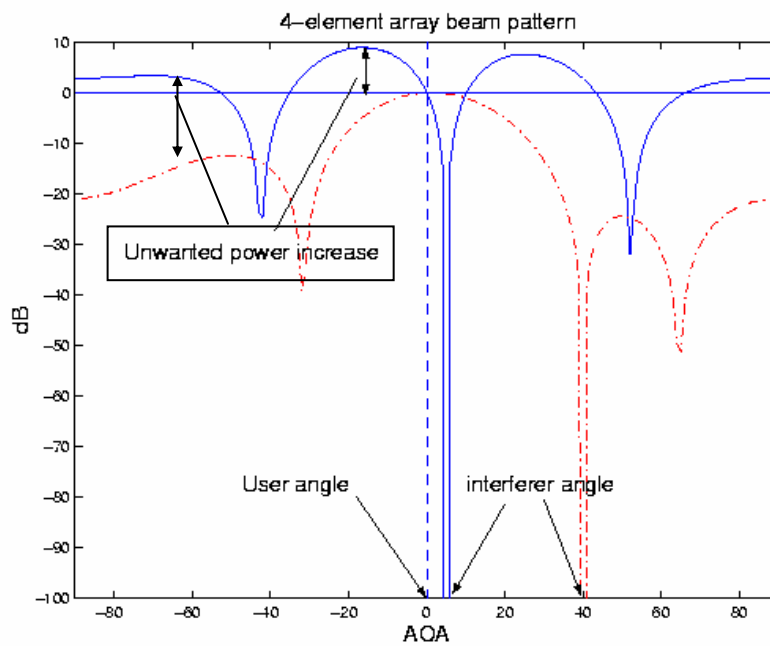


Figure 17 The beam patterns of a 4-element linear array using zero-forcing beamforming. The DOA (angle of arrival) of the desired user is at 0° (broadside angle) and the interferer is moving from 40° (dash-dot) to 5° (solid). The overshoot of the main lobe is approximately 9 dB.

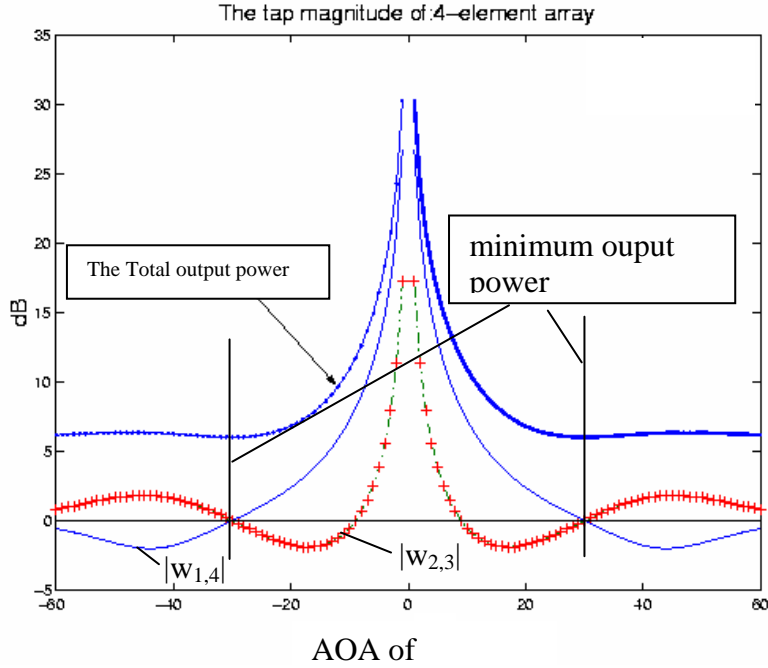


Figure 18 The variation of magnitude of the taps of the 4-element array (zero-forcing beamformer) when the desired user DOA is fixed at 0° and the interferer DOA (null position) swings from -60° to $+60^\circ$. (note that the 1st and the 4th tap have the same magnitude and increase tremendously when the separation angle becomes small)

3.2 Zero-forcing beamformer

In the zero-forcing beamforming method, the optimum weight vector is basically a minimum solution for a linear system, which is constrained by predetermined array responses at the desired and the cochannel users directions. The number of total users is assumed to be less than or equal the number of array elements. Consider an N -element linear uniform array with L signal sources. Assume that θ_1 is the DOA of the desired user where unity response is required and $\theta_2, \theta_3, \dots, \theta_L$ are DOAs of cochannel users where nulls are required. The steering vectors $\mathbf{a}(\theta_i)$ $i=1,2,\dots,L$ are given by

$$\mathbf{a}(\theta) = \begin{bmatrix} 1 & e^{j\left[\frac{2\pi d}{\lambda} \sin \theta\right]} & e^{j\left[\frac{4\pi d}{\lambda} \sin \theta\right]} & \dots & e^{j\left[\frac{2\pi d}{\lambda} (N-1) \sin \theta\right]} \end{bmatrix}^T \quad (44)$$

The optimum weight vector for the zero-forcing beamformer, \mathbf{w}_z , is the solution of the following simultaneous equations:

$$\begin{cases} \mathbf{w}_z^H \mathbf{a}(\theta_1) = 1 \\ \mathbf{w}_z^H \mathbf{a}(\theta_2) = 0 \\ \dots \\ \mathbf{w}_z^H \mathbf{a}(\theta_L) = 0 \end{cases} \quad (45)$$

Using matrix notation, (45) becomes:

$$\mathbf{w}_z^H \mathbf{A} = \mathbf{f}^T \text{ or } \mathbf{A}^H \mathbf{w}_z = \mathbf{f} \quad (46)$$

where $\mathbf{A} = [\mathbf{a}(\theta_1) \mathbf{a}(\theta_2) \dots \mathbf{a}(\theta_{L-1}) \mathbf{a}(\theta_L)]$ is the array manifold, consisting of all L steering vectors of L directional sources and $\mathbf{f} = [1 \ 0 \ \dots \ 0]^T$ is a constraint vector consisting of the array response at each source direction. The $(\cdot)^T$ and $(\cdot)^H$ denote the transpose and conjugate transpose respectively. If $L=N$ (the number of users is equal to the number of array elements), assuming that all steering vectors are linearly independent, the matrix A is invertible and thus (46) has a unique solution shown in (47):

$$\mathbf{w}_z = \mathbf{A}^{-1} \mathbf{f} \quad (47)$$

If $L < N$ (the number of users is less than the number of array elements), the matrix A is noninvertible and (46) is overdetermined. Using *min norm* theorem [20], the minimum solution in this case is:

$$\mathbf{w}_z = \mathbf{A}(\mathbf{A}^H \mathbf{A})^{-1} \mathbf{f} \quad (48)$$

The drawback of the zero-forcing beamformer is its sensitivity to the direction of nulls. Zero-forcing beamformers form very narrow and deep nulls towards the estimated DOAs of cochannel users. If the estimated null directions were inaccurate (a few degrees error) then the null depths in the real cochannel users directions decrease very fast causing a

decrease in the SIR (Signal-to-Interference-Ratio). Also in the practical urban scattering environment, angular spread (caused by refraction or reflection from surrounding objects) of up to 15° has been measured [22] and this results in null filling (i.e. forming shallow null) in the array radiation pattern. In these practical situations infinite nulls never occur. In addition the terminal receiver experiences noise and co-channel interference from many other basestations and that produces a floor below which attenuation of an interfering signal has little value. Therefore, a deliberate reduction of the null depth can be used to improve the power requirement of the array without sacrificing too much interference performance in the co-channel directions.

3.3 Output power reduction by changing the null depth

3.3.1 Global minimum of the output power surface

As mentioned in 3.3, the optimum weight of the zero-forcing beamformer is the minimum solution of the linear system (48).

The total power P can be expressed as:

$$P = \|\mathbf{w}_z\|^2 = \mathbf{w}_z^H \mathbf{w}_z = \sum_{i=1}^N |w_i|^2 \quad (49)$$

Substituting (48) into (49) gives:

$$P = (\mathbf{A}(\mathbf{A}^H \mathbf{A})^{-1} \mathbf{f})^H \mathbf{A}(\mathbf{A}^H \mathbf{A})^{-1} \mathbf{f} = \mathbf{f}^H (\mathbf{A}^H \mathbf{A})^{-1} \mathbf{f} \quad (50)$$

If the constraint vector, \mathbf{f} , is modified then the output power will be changed accordingly.

If the components of the \mathbf{f} vector become non-zero, $\mathbf{f} = [f_1 \ f_2 \ \dots \ f_L]^T$, where $f_i = |f_i| e^{j\phi_i}$ ($i=1,2,\dots,L$) then the value of $|f_i|$ will determine the null depth and the $\arg(f_i)=\phi_i$ represents the phase of the residue signal in the null direction. This phase has no effect on system performance and therefore ϕ_i is chosen in the range $-\pi$ to $+\pi$ to minimise the array

output power $P(\mathbf{f})$. The null depths, $|f_i|$, $i=1,2, \dots,L$, are assumed known and set in advance to less than a certain level, δ_i , using the expected SIR requirement of the co-channel users. The system in (48) becomes:

$$\begin{cases} \mathbf{w}^H \mathbf{a}(\theta_1) = f_1 \\ \mathbf{w}^H \mathbf{a}(\theta_2) = f_2 \\ \dots \\ \mathbf{w}^H \mathbf{a}(\theta_L) = f_L \end{cases} \quad (51)$$

The output power, $P(\mathbf{f}) = \mathbf{f}^H (\mathbf{A}^H \mathbf{A})^{-1} \mathbf{f}$ which is a quadratic function of the constraint vector, \mathbf{f} , can be minimised with respect to \mathbf{f} . The optimisation problem can be expressed as:

$$\text{minimize } P(\mathbf{f}) = \mathbf{f}^H (\mathbf{A}^H \mathbf{A})^{-1} \mathbf{f} \quad \text{subject to } \begin{cases} f_1 = \delta_1 \\ 0 < |f_2| \leq \delta_2 \\ \dots \\ 0 < |f_L| \leq \delta_L \end{cases} \quad (52)$$

where: δ_1 is the predetermined look direction response (equal 1) and $\delta_2, \dots, \delta_L$ are and null depths of the output pattern. The main idea of the null depth control technique is to *find the optimum value of the components f_i of the constraint vector \mathbf{f} in a certain region*

$0 < |f_i| < \delta_i$ ($i=2, \dots, L$) so that the output power P is minimum. This is an optimisation problem with inequality constraints. Finding the general solution for this problem is rather difficult.

In order to study the effect of ϕ_i on the array transmit power, a brute-force calculation was performed.

Figure 19 shows how the output power from a 4-element array varies with ϕ_i for a single null lying 10^0 off the broadside look direction. The effect of different null depths is shown. A perfect null, $|f_2|=0$, requires 5 dB extra transmit power and is not affected by ϕ_i . As the null depth increases the extra transmitted power can be reduced with the correct choice of ϕ_i . The minimum transmit power of 0 dB is obtained when the null depth is set

to the natural response level of a beamforming without null steering. However, the phase of ϕ_i for minimum power remains the same, $\phi_i = \phi_{opt}$, for all null depths. The next section will prove that the optimum phase of the residue null signal, ϕ_i , is only dependant on the DOA of the signals. This also applies to the multiple null scenarios.

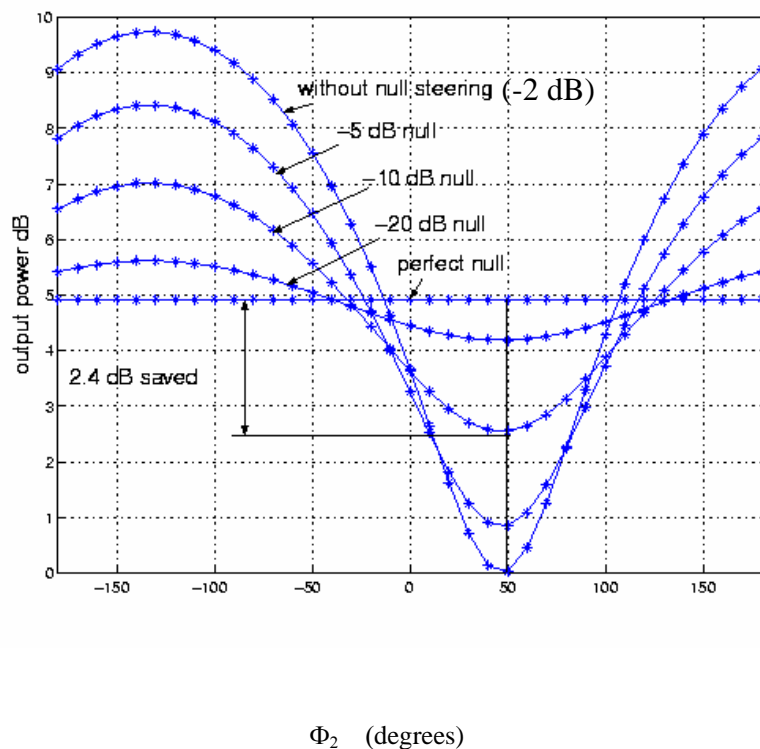


Figure 19 The output power variation with respect to ϕ_2 the phase of the residual signal in the null direction. Null depths are $-\infty$, -20 dB, -10 dB, -5 dB, and -2 dB. The array has 4 elements, one desired user at broadside angle, one interferer at 10 degrees.

3.3.2 Minimum of the output power by varying ϕ .

In this approach we reduce the complexity of the optimisation problem by using equality constraints for the magnitude, and then optimising the phase, ϕ_i , for minimum power.

Equation (52) can be rewritten as:

$$\text{minimize } P(\mathbf{f}) = \mathbf{f}^H (\mathbf{A}^H \mathbf{A})^{-1} \mathbf{f} \quad \text{subject to} \quad \begin{cases} f_1 = |f_1| e^{j\phi_1} \\ f_2 = |f_2| e^{j\phi_2} \\ f_i = |f_i| e^{j\phi_i} \quad \text{where } -\pi < \phi_i < +\pi \\ \dots \\ f_L = |f_L| e^{j\phi_L} \end{cases} \quad (53)$$

Let $\mathbf{K} = (\mathbf{A}^H \mathbf{A})^{-1}$ and $f_l = |f_l| e^{j\phi_l} = 1$ is the look direction response. The minimisation of P can be achieved by varying the angle ϕ_i . The differential equation is:

$$\begin{cases} \frac{\partial P(\phi_2)}{\partial \phi_2} = 0 \\ \frac{\partial P(\phi_3)}{\partial \phi_3} = 0 \\ \dots \\ \frac{\partial P(\phi_L)}{\partial \phi_L} = 0 \end{cases} \quad (54)$$

The partial differentiation of (54) can be expanded for $2 < i < L$

$$\frac{\partial P(\phi_i)}{\partial \phi_i} = \frac{\partial (\mathbf{f}^H \mathbf{K} \mathbf{f})}{\partial \phi_i} = \frac{\partial \mathbf{f}^H}{\partial \phi_i} \mathbf{K} \mathbf{f} + \mathbf{f}^H \mathbf{K} \frac{\partial \mathbf{f}}{\partial \phi_i} = 0 \quad (55)$$

the vector \mathbf{f} can be written as:

$$\mathbf{f} = [|f_1| e^{j\phi_1}, \dots, |f_i| e^{j\phi_i}, \dots, |f_L| e^{j\phi_L}]^T \quad \text{and} \quad \mathbf{f}^H = [|f_1| e^{-j\phi_1}, \dots, |f_i| e^{-j\phi_i}, \dots, |f_L| e^{-j\phi_L}] \quad (56)$$

The partial derivative provides:

$$\frac{\partial \mathbf{f}}{\partial \phi_i} = j[0, \dots, |f_i| e^{j\phi_i}, \dots, 0]^T \quad \text{and} \quad \frac{\partial \mathbf{f}^H}{\partial \phi_i} = -j[0, \dots, |f_i| e^{-j\phi_i}, \dots, 0] \quad (57)$$

substituting (57) into (55) yields:

$$-j[0, \dots, |f_i| e^{-j\phi_i}, \dots, 0] \mathbf{K} [|f_1| e^{j\phi_1}, \dots, |f_i| e^{j\phi_i}, \dots, |f_L| e^{j\phi_L}]^T + \quad (58)$$

$$j[|f_1| e^{-j\phi_1}, \dots, |f_i| e^{-j\phi_i}, \dots, |f_L| e^{-j\phi_L}] \mathbf{K} [0, \dots, |f_i| e^{j\phi_i}, \dots, 0]^T = 0$$

$$-|f_i| e^{-j\phi_i} \mathbf{K}_{i,1 \dots L} [|f_1| e^{j\phi_1}, \dots, |f_i| e^{j\phi_i}, \dots, |f_L| e^{j\phi_L}]^T + \quad (59)$$

$$[|f_1|e^{-j\phi_1}, \dots, |f_i|e^{-j\phi_i}, \dots, |f_L|e^{-j\phi_L}] \mathbf{K}_{1\dots L,i} |f_i|e^{j\phi_i} = 0$$

where $\mathbf{K}_{m,n}$ denotes the element of the matrix \mathbf{K} at the m -th row and n -th column. The row and column vector $\mathbf{K}_{i,1..L} = [\mathbf{K}_{i,1} \mathbf{K}_{i,2} \dots \mathbf{K}_{i,L}]$ and $\mathbf{K}_{1\dots L,i} = [\mathbf{K}_{1,i} \mathbf{K}_{2,i} \dots \mathbf{K}_{L,i}]^T$ are extracted from \mathbf{K} . The equation (59) can be rewritten as:

$$-j|f_i|e^{-j\phi_i} \left(\sum_{k=1}^L \mathbf{K}_{i,k} |f_k| e^{j\phi_k} \right) + j|f_i|e^{j\phi_i} \left(\sum_{k=1}^L \mathbf{K}_{k,i} |f_k| e^{-j\phi_k} \right) = 0 \quad (60)$$

the (60) can be simplified as:

$$j|f_i| \sum_{k=1}^L |f_k| (-\mathbf{K}_{i,k} e^{j(\phi_k - \phi_i)} + \mathbf{K}_{k,i} e^{j(\phi_i - \phi_k)}) = 0 \quad (61)$$

The solution of (61) can be obtained when:

$$\mathbf{K}_{i,k} e^{j(\phi_k - \phi_i)} = \mathbf{K}_{k,i} e^{j(\phi_i - \phi_k)} \quad \text{or} \quad e^{2j(\phi_i - \phi_k)} = \frac{\mathbf{K}_{i,k}}{\mathbf{K}_{k,i}} \quad \text{for } k=1, \dots, L. \text{ and } 2 \leq i \leq L \quad (62)$$

noting that $\phi_1=0$ (the look direction response), (62) can be written as:

$$\begin{cases} \phi_1 - \phi_1 = \arg\{\mathbf{K}_{i,1}\} \\ \phi_1 - \phi_2 = \arg\{\mathbf{K}_{i,2}\} \\ \dots \\ \phi_1 - \phi_L = \arg\{\mathbf{K}_{i,L}\} \end{cases} \quad \text{for } 2 \leq i \leq L, \text{ and this means:} \quad (63)$$

$$\begin{cases} \phi_1 = \arg\{\mathbf{K}_{i,1}\} \\ \phi_2 = \arg\{\mathbf{K}_{i,1}\} - \arg\{\mathbf{K}_{i,2}\} \\ \dots \\ \phi_L = \arg\{\mathbf{K}_{i,1}\} - \arg\{\mathbf{K}_{i,L}\} \end{cases}$$

Because the matrix, \mathbf{K} , is a symmetrical matrix: $\mathbf{K}=\mathbf{K}^H$ then: $\mathbf{K}_{i,j} = \mathbf{K}_{j,i}^*$. We can also show (by a brute force evaluation of the elements \mathbf{K}_{ij}) that the following relationships between the elements of \mathbf{K} , holds: (the proof is not included in this thesis).

$$\arg\{\mathbf{K}_{i,j}\} - \arg\{\mathbf{K}_{k,j}\} = \arg\{\mathbf{K}_{i,k}\} \quad (64)$$

From this special property, the optimum phase, ϕ_i , from equation (63) is a unique solution of the system in (54) :

$$\begin{cases} \phi_2 = \arg\{\mathbf{K}_{2,1}\} \pm n\pi \\ \dots \\ \phi_i = \arg\{\mathbf{K}_{i,1}\} \pm n\pi \text{ where } n = 0, 1, 2, \dots \\ \dots \\ \phi_L = \arg\{\mathbf{K}_{L,1}\} \pm n\pi \end{cases} \quad (65)$$

In order to prove that this is a minimum point, we can use the second order derivative of P (from equations (61))

$$\frac{\partial P^2(\phi_i)}{\partial \phi_i^2} = -|f_i| \sum_{k=1}^L |f_k| (\mathbf{K}_{i,k} e^{j(\phi_k - \phi_i)} + \mathbf{K}_{k,i} e^{j(\phi_i - \phi_k)}) \quad (66)$$

From (64) and (65) we have $\arg\{\mathbf{K}_{i,k}\} = (\phi_i - \phi_k)$ and $|\mathbf{K}_{k,i}| = |\mathbf{K}_{i,k}|$ therefore (66) becomes:

$$\begin{aligned} \frac{\partial P^2(\phi_i)}{\partial \phi_i^2} &= -2|f_i| \|f_k\| |\mathbf{K}_{i,k}| e^{jn\pi} \\ &= \begin{cases} 2|f_i| \|f_k\| |\mathbf{K}_{i,k}| > 0 & \text{if } \phi_i = \arg\{\mathbf{K}_{i,1}\} \pm 2(n+1)\pi \quad (\text{min}) \\ -2|f_i| \|f_k\| |\mathbf{K}_{i,k}| < 0 & \text{if } \phi_i = \arg\{\mathbf{K}_{i,1}\} \pm 2n\pi \quad (\text{max}) \end{cases} \end{aligned} \quad (67)$$

Equation (67) shows that there exists a phase angle, $\phi_i = \arg\{\mathbf{K}_{i,1}\} \pm 2(n+1)\pi$ of the complex displacement f_i at which the output power P is minimum. From this point, it is necessary to emphasise that with predetermined null depths of any value $|f_i|$, it is possible to reduce the array output power by setting the phase of the complex displacement, f_i , to ϕ_i using (65). This phase, ϕ_i is independent of the null depth specification $|f_i|$, and can be pre-calculated from the DOA information.

Figure 20 shows the quadratic surface of the output power of a 3-elements antenna array in the 3D plot with respect to variation of phase and magnitude of complex displacement δ . The lowest point of this surface corresponds to the inactive minimum output power (no null steering). Keep moving along $|\delta|$ direction, there are the minimum output power points correspond to optimum phase ϕ . This figure shows that: the variation of $|\delta|$ implies

the variation of null depth in the look direction and thus the reduction of the output power of the array can be obtained.

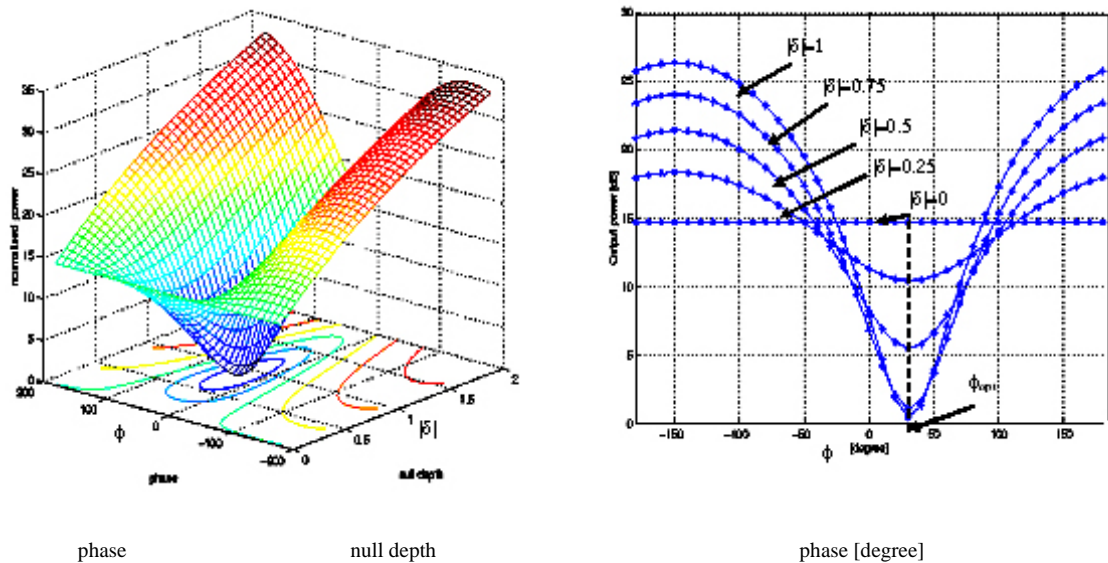


Figure 20 (a) The output power surface of the 3-element array with respect to magnitude and phase of the displacement δ . (b) The cross-sectional of the power surface at different values of $|\delta|$. When $|\delta| = 0$, the array has infinite null at the look direction and therefore no optimum phase can be obtained to minimize the output power.

3.3.3 Algorithm for output power reduction by trading off the null depth

Since the optimum displacement phases, $\phi_i, i=2,3,\dots,L$, are known, then the minimum transmitted power is obtained from (52). This is still a difficult problem to solve. Since it is not possible to use the *min-norm* theorem of (52) directly, which requires equality constraints, we use it in an indirect manner. Figure 21 shows an algorithm for obtaining minimum output power using the min-norm theorem with maximum null depth constraints.

The description of the algorithm for 2 null design is as follows: (see Figure 21)

- Design beamformer without null steering, $\mathbf{f}=1$.

- Check if the no-null steering beam pattern satisfies the null depth requirements. If so, use the no-null steering design.
- Design beamformer with single null of given depth, repeat for all of null positions $\mathbf{f}_i = [1, \delta_i e^{j\phi_i}]^T, i=2, \dots, L$ where $L=3$ in this example.
- Check if any of the single null beamformer satisfies null depth requirements. If so use the single beamformer with the lowest power, otherwise:
- Design beamformer with two nulls of given depths repeat for all null combinations, $\mathbf{f} = [1, \delta_j e^{j\phi_j}, \delta_k e^{j\phi_k}]^T, j \neq k = 2, \dots, L$ where $j=3; k=2$ in this example.

The first two steps of the algorithm check to see if the required nulls fall within the natural null positions of the simple beamformer (without null steering), which represents the minimum transmit power condition and the maximum degrees of freedom. As the algorithm proceeds the degree of freedom are decreased, one by one, by fixing an increasing number of null depths. The algorithm can be extended for nulls greater than 2 but get tedious when the number of nulls is large.

In the next section we use this algorithm to study the statistical performance of a null steering adaptive array.

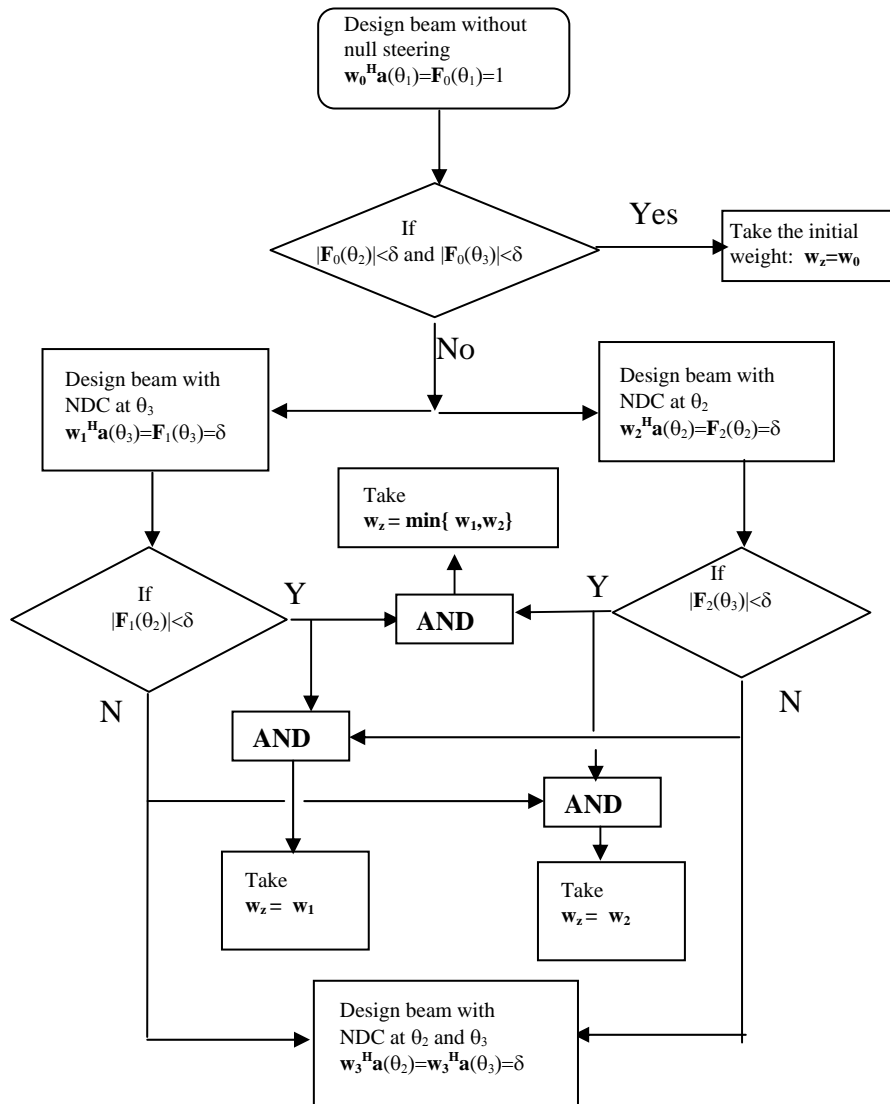


Figure 21 The flow diagram of the algorithm for designing antenna array weights with minimum output power. (4-element array, one user and two interferers)

4 Numerical verification and simulation results

4.1 Trade off null depth for the output power reduction

Figure 22 shows the relationship between array output power and null depth for different separation angles between the desired (broadside) and a single interferer direction ($\theta_s=10^\circ, 15^\circ, 20^\circ$). The same array as in the previous example has been investigated. The plots indicate that when the separation angle is small, the null depth control can save a significant amount of transmit power. (approximately 2.4 dB for the case of 10° separation angle and a -10dB null depth).

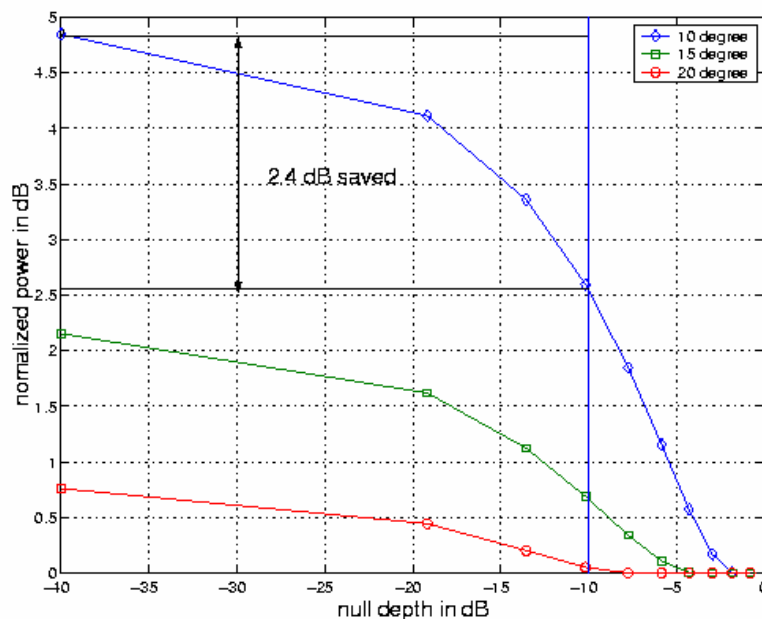


Figure 22 The output power curve versus the null depth for different separation angle of $10^\circ, 15^\circ, 20^\circ$

4.2 Power constraints for a linear array

Figure 23 shows two methods of powering an adaptive array. The first uses a separate amplifier to power each antenna element, the second uses a distributed amplifier arrangement where the input signal passed through a Butler or other similar matrix before

reaching the antennas [24]. In this way, a signal on input port n is distributed across all N amplifiers and then combined in the inverse matrix to feed antenna n . None of this signal appears on the other antennas. All amplifiers handle equal power even when each antenna element is driven at a different output power level. The matrix allows for power equalisation across the amplifiers, but has an associated insertion loss, which will force a slightly high power rating overall. The minimum output power of the array is the primary constraint for beamforming algorithms. On the other hand, the power distribution among the array elements is greatly non-uniform therefore, a secondary constraint that applies to for systems using the architecture of figure 23a is to minimise the size of the power amplifiers attached to each element. In addition, the objective is to maximise the probability that the array will handle the required beamforming and null steering without resorting to intracell handovers. To achieve this, one shall consider a uniform angular traffic distribution for desired and co-channel users over a 120° sector (Figure 24). It is necessary to calculate the additional transmit power required to handle a number of nulls at a certain probability level by scanning the main beam of the desired and the nulls of the co-channel users to cover all angular possibilities (in 1° steps). In the following section, a sequence of simulations will show the performance of a 4-element array steering 1 or 2 nulls.

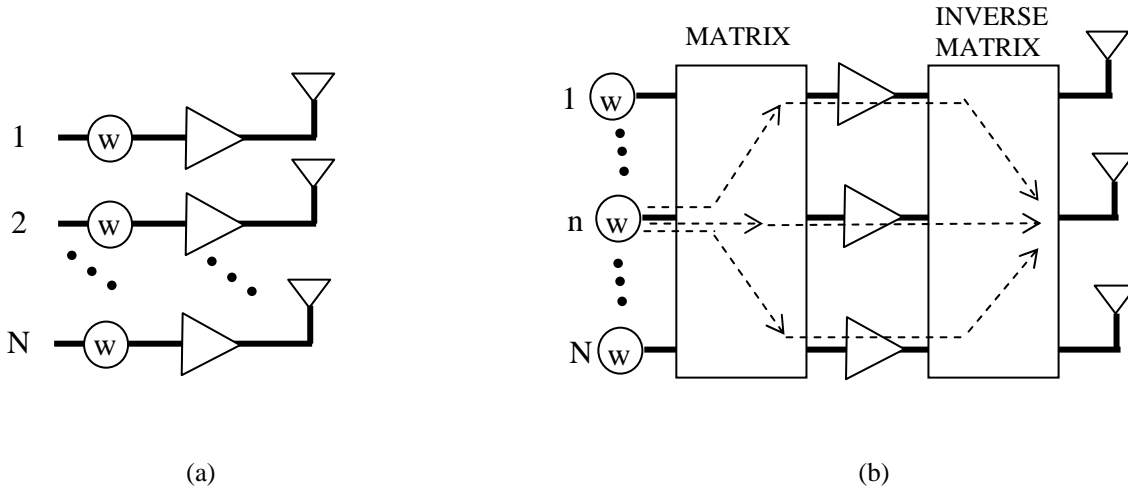


Figure 23 Two schemes of powering an antenna array: (a) Separate power amplifiers feeding elements (b) Distributed power amplifiers using Butler (or other similar) matrix and inverse matrix.

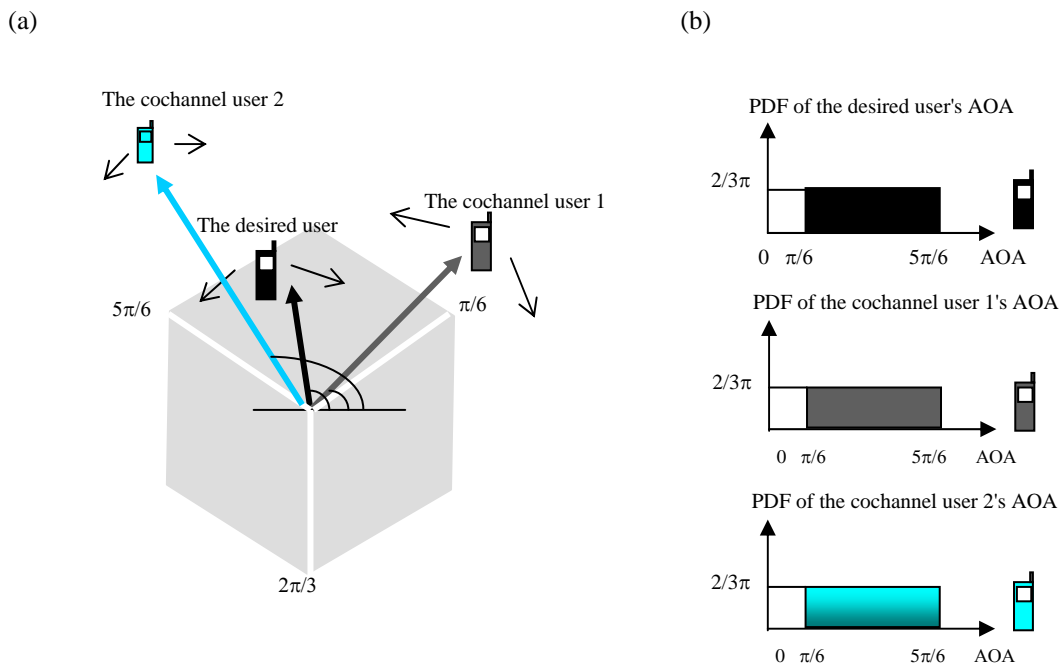


Figure 24 (a) The relative angular positions of desired and cochannel users composes an angular scenario. (b) The PDF of the desired and cochannel user (equiprobable)

4.3 Additional transmit power for null steering

The amount of additional transmit power required for null steering depends on the relative angular locations of the desired and interfering users. Figure 25 and 26 plots the fraction of angular scenarios that the adaptive antenna can handle for a given increase in transmit power (based on uniform angular distributions for both look and null directions), when steering only a single null (fig. 25). The additional power required is minimal (0.6 dB) for 63 % of angular scenarios with an infinite null. This increase to 72.5% of scenarios when the null depth is relaxed to -10 dB. If we allow greater transmit power, say up to 3 dB, the respective figure are 75 % and 82 %. In this case, relaxing the null depth only increases array null steering capability by 7 %.

The situation deteriorates rapidly when 2 nulls are required (fig. 26). If only a small increase in transmit power is allowed (0.6 dB) then the array's ability to steer infinite nulls drops to 25 %. An array with such a low performance would not be practical since the channel allocation problem would be extremely difficult and force an unnecessary high level of handovers. The performance can be vastly improved (to 50 %) by relaxing null depth to -10 dB. The corresponding figures for 3 dB additional transmit power are 50 % and 66 %. In both one and two null cases, the effectiveness of relaxing the null depth is greatest when the additional transmit power of the array is restricted to small values.

The above performance limits apply to arrays using the distributed amplifier technique (Figure 23b), where the transmit power is shared equally among the amplifiers. However, figures 25 and 26 can not be used for the traditional transmit architecture because they do not show how the power is distributed among the antenna elements. The next section considers the power distribution between the taps.

4.4 Power distribution between the antenna elements

4.4.1 Scenario of one user and one interferer

Designs using the *min norm* theorem always end up with symmetrical tap magnitudes (ie $|w_1|=|w_N|$; $|w_2|=|w_{N-1}|$; ...etc) and so only two taps need to be considered when $N=4$. Figure 27a and b show a scatter diagram of the tap power for single null with ∞ dB and -10 dB null depths. The tap magnitudes are correlated and fall on a single line. At large transmit powers the relationship between the taps is almost linear. To cover all scenarios that require up to 3 dB additional transmit power, the amplifier for the inner tap, $w_{2,4}$, must have $(0.32/0.25)^2 = 1.64$ times increased power rating, while the amplifier for the outer taps, $w_{1,3}$, should have $(0.45/0.25)^2 = 3.24$ times increased power rating. Note that tap magnitudes of 0.25 represent the no null steering and minimum transmit power conditions. Hence this point falls on the 0dB power contour. The power amplifiers (PA) for the inner elements need not be as large as the PA's on the outer elements but the power rating for the entire antenna array must be increased to $10\log_{10}(2(0.32^2+0.45^2)/4(0.25)^2) = 3.8$ dB. This is more than the 3 dB additional transmit power needed by the distributed amplifier and is because maximum power is not reached on each element simultaneously. Reducing the null depth to -10 dB results in a lower transmission power for the two inside elements ($|w_{2,3}| = 0.25$ see figure 27) and a greater antenna utilities of 82% and 68% (up from 76% and 50%, see figure 25 and 26)

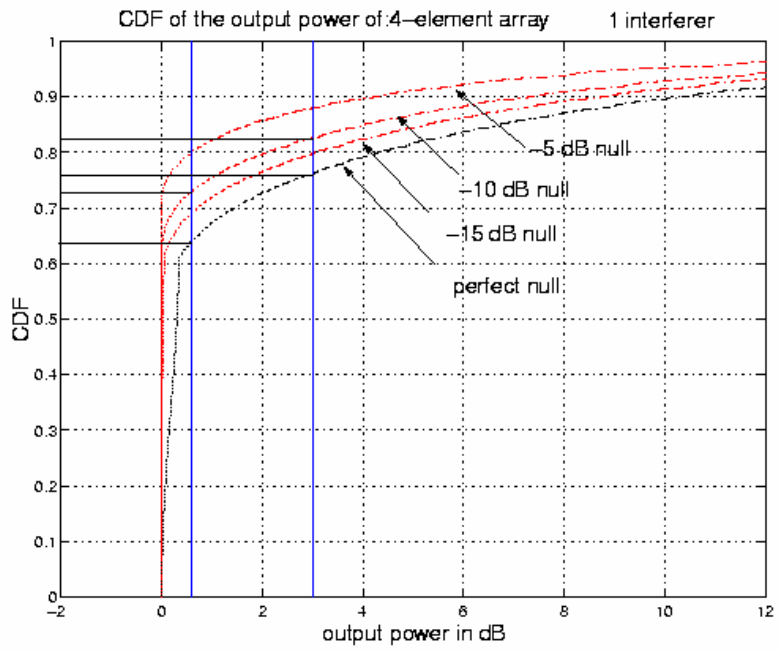


Figure 25 The CDF of the output power of the 4-element array with different null depths (∞ , -15 dB, -10 dB, and -5 dB) for the case of *one user and one interferer*.

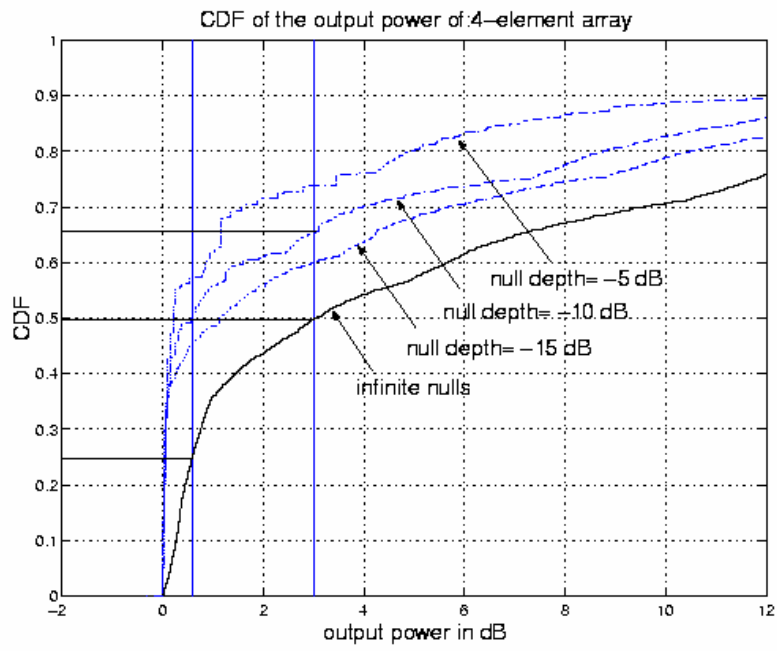


Figure 26 The CDF of the output power of the 4-element array with different null depths (∞ , -15 dB, -10dB, and -5dB) for the case of one user and two interferers.

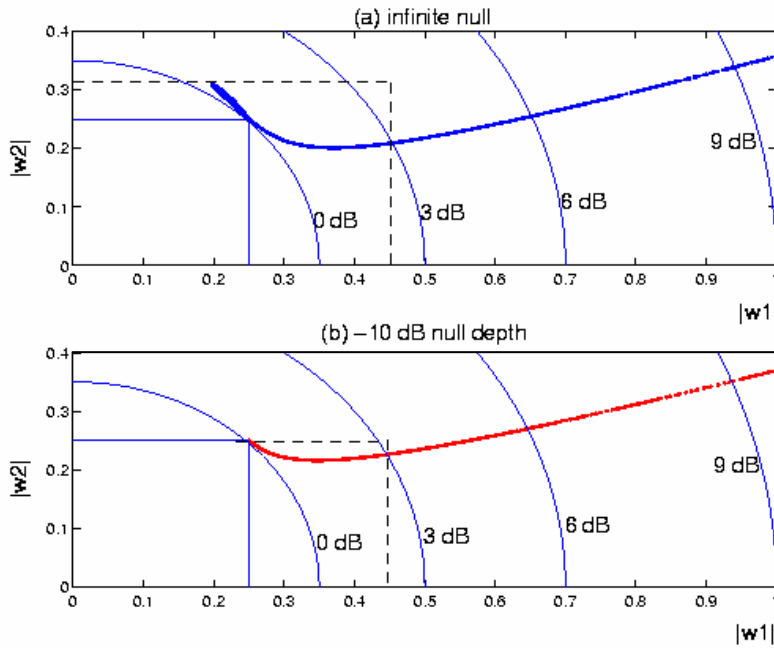


Figure 27 Relationship between the magnitude of the taps for a 4-element array in the case of one user and one interferer. (a) Array steers a perfect null. (b) When the array steers a null of -10 dB depth. Contours of constant power are shown.

4.4.2 Scenario of one user and two interferers

Figure 28 shows a scatter plot describing the relationship between the taps when two infinite nulls are required. Correlation between the taps is now not so obvious and it is no longer possible to identify the power ratio that will cover the maximum number of the user scenarios. The joint Cumulative Distribution Function $P(|w_1| < x; |w_2| < y)$, represented by the contours, is shown in Figure 29 and 30. This can be used to determine the tap ratios for a maximum antenna performance. The optimum tap values follow the sharp ridge (shown by the dotted line in figure 30) since it crosses the CDF contours at the minimum power rating of the amplifier. On this figure, the curves of constant additional power represent the combined power rating of the amplifiers. For a given CDF value this is greater than the power required in figure 26. For example: 50 % of user scenarios need

3dB extra transmit power (fig. 26), (distributed amplifier) but the individual antenna elements, $w_{1,4}$ and $w_{2,3}$ must increase by $(0.42/0.25)^2$ and $(0.4/0.25)^2$ respectively, (the intersection of the dash lines in figure 29). The total power rating of the antenna is now increased to $10\log_{10}(2(0.42^2+0.4^2)/4(0.25)^2) = 4.3$ dB; this is 1.3 dB more than would be required by the distributed amplifier solution. Figure 30 shows the CDF contour for -10 dB null depths. The array rating is now increase by only $10\log_{10}((2(0.31^2+0.27^2)/4(0.25)^2) = 1.3$ dB for a CDF = 50 %. (the intersection of the dash lines in figure 30).

The additional power rating comparison of the separate PA and distributed PA is summarised in the following tables for two antenna performances (utilities) CDF=50 % and CDF=70 %. The figures for the separate amplifier system show the composite power increases as well as the power increase of each antenna element, $|w_{1,4}|$ and $|w_{2,3}|$.

Number of nulls required	Additional transmit power rating required for the CDF of 50 % of angular scenarios			
	Distributed amplifier system (fig. 23b) (all PA's are equal)		Separate amplifier system (fig. 23a) ($ w_{1,4} \neq w_{2,3} $)	
	Null depth = $-\infty$	null depth = -10 dB	null depth = $-\infty$	null depth = -10 dB
1 null	0.3 dB (fig 25)	0 dB (fig 25)	1.65 dB (fig 27a) $ w_{1,4} =1.7\text{dB};$ $ w_{2,3} =1.6\text{dB}$	0 dB (fig 27b) $ w_{1,4} =0\text{dB};$ $ w_{2,3} =0\text{dB}$
2 nulls	3 dB (fig 26)	0.6 dB (fig 26)	4.3 dB (fig 29) $ w_{1,4} =4.6\text{dB};$ $ w_{2,3} =4.1\text{dB}$	1.1 dB (fig 30) $ w_{1,4} =1.6\text{dB};$ $ w_{2,3} =0.5\text{dB}$

(a)

Number of nulls required	Additional transmit power rating required for the CDF of 70 % of angular scenarios			
	Distributed amplifier system (fig. 23b)		Separate amplifier system (fig. 23a)	
	null depth = $-\infty$	null depth = -10 dB	null depth = $-\infty$	null depth = -10 dB
1 null	1.5 dB (fig 25)	0.22 dB (fig 25)	2.7 dB (fig 27a) $ w_{1,4} =3.3\text{dB};$ $ w_{2,3} =1.9\text{dB}$	0.7 dB (fig 27b) $ w_{1,4} =1.3\text{dB};$ $ w_{2,3} =0\text{dB}$
2 nulls	9.6 dB (fig 26)	4 dB (fig 26)	10.7 dB (fig 29) $ w_{1,4} =11.5\text{dB};$ $ w_{2,3} =9.2\text{dB}$	4.65 dB (fig 30) $ w_{1,4} =6.1\text{dB};$ $ w_{2,3} =3.2\text{dB}$

(b)

Table 2: Additional transmit power rating required :

(a) for the CDF of 50 % of angular scenarios

(b) for the CDF of 70 % of angular scenarios

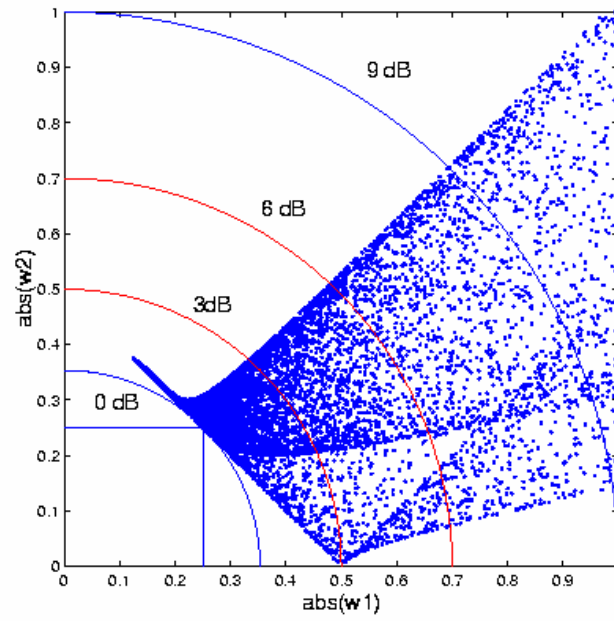


Figure 28 Relationship between the magnitude of the taps for a 4-element array in the case of *one user and two interferers*. Contours of constant power are shown. The null depths are *infinity*.

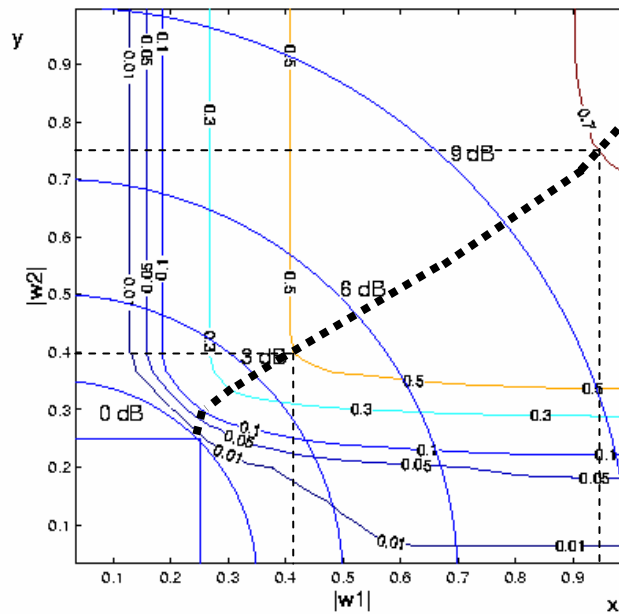


Figure 29 The plot of the joint CDF of the output power, $P(|w_1| < x; |w_2| < y)$, of the 4-element array in the case of *one user and two interferers*. The null depths are *infinity*.

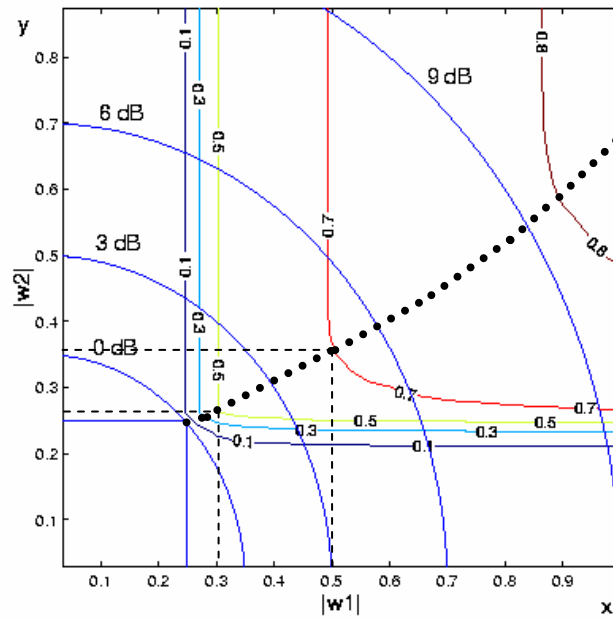


Figure 30 The plot of the joint CDF of the output power, $P(|w_1| < x; |w_2| < y)$, of the 4-element array in the case of *one user and two interferers* with the null depths ≤ -10 dB. Antenna performance (utility) is significantly improved.

5 Conclusion

The *min norm* technique for designing zero-forcing beamformer from angle of arrival information can be modified to design beams containing nulls with arbitrary magnitude constraints. The modification exploits the property that the phase of the residual signal at the null angle has an optimum value for minimum transmit power, and is determined by the spatial information. This simplifies the constraint vector, f , and allows the *min norm* routine to be embedded in a simple algorithm to calculate the antenna weights that results in minimum transmit power.

From the investigation on the performance of a 4 element array using modified *min-norm* beamforming method, the following concluding remarks can be made:

- Null steering causes transmit power to increase particularly when nulls are spatially close to the desired signal. The more nulls that are steered, the greater the power increases. A single null system has a power penalty of 1.5 dB rising to 9.6 dB for two nulls (at 70% utility). The latter figure would be unacceptable in any practical system. It can be reduced to 4 dB by allowing a reduced null depth of -10 dB.
- Constraints on the transmit power, amplifier size and additional interference in the non-steered direction limit the utility of adaptive antennas to certain angular scenarios. Hence, the system must carefully control channel allocation to avoid high power and high interference conditions.
- The utility of an adaptive antenna system can be improved by relaxing the null depths. A null of -10 dB can increase the utility of the antenna from 76 % to 82 % (single null condition) and from 50 % to 67 % (two null condition) when the antenna system transmits up to 3 dB extra power.

- Antennas with null steering algorithms require non-uniform output power on the antenna elements. The outer elements generally require more power, and the amplifier on those elements should have a higher power rating.

Distributed amplifiers can lead to a small reduction in the total amplifier power rating of less than 0.9 dB for -10 dB nulls and up to 1.35 dB for perfect nulls. The additional losses of the splitting/ combining matrix are likely to cancel much of this improvement.

However, they remove the need for amplifiers with different power ratings which the simulation shows can be as high as 2.9 dB and for this reason distributed amplifiers would be the preferred architecture for null steering adaptive antenna systems.

6 Summary of Significance

The use of the adaptive antenna array to improve the capacity and quality of service of the cellular radio system undoubtedly is a vital part of 3G wireless technologies. This thesis is to improve the performance of adaptive antennas in the "difficult" situation where there is low angular separation between desired and undesired users, and therefore it pushes the smart antennas technology closer to worldwide deployment for the third generation of wireless communication and beyond. The results of this research contribute to the benefit of using adaptive antennas. These benefits can be summarised as follows:

- *Coverage range:* Adaptive antenna arrays can increase the cell coverage range substantially through antenna gain and interference rejection. In particular, the coverage range can be improved by a factor of $N^{1/n}$, where N denotes the number of elements and n denotes the propagation loss exponent.
- *Capacity:* Adaptive antenna arrays can increase the number of voice channels through the use of a directional communication link. The increase factor depends on the propagation environment and the number of antenna elements. The point is that it is possible to have multiple mobiles on the same RF channel but different spatial channel at a particular cell site. Adaptive antennas are expected to play an important role in enhancing 3G systems: particularly in a multi-rate traffic scenario. High data rate users would be "nulled out" reducing their ability to overload the cell.
- *Signal quality:* Adaptive antenna arrays can be considered as spatial equalizers and can provide substantial signal quality improvements through spatial signal processing. In fact, some implementations of adaptive antennas provide a spatial RAKE receiver capability to combine uplink multipath arrivals for improved output SIR.
- *Reduction of expenses:* In the downlink, adaptive antenna arrays focus the energy sent out into the cell. This lower the power requirements and gives a decrease in the size of

the power amplifiers required at the base station. Lower amplifier costs, power consumption, and higher reliability will result in an overall reduction in costs of using wireless technology.

REFERENCES

- [1] M. Barrett and R. Arnott, "Adaptive antennas for mobile communications".
Electronics & Communications Eng. Journal, vol. 6, pp. 203-214, Aug. 1994.
- [2] W.C. Lee, "Mobile Cellular Telecommunications", *McGraw-Hill*, 1995.
- [3] H. Krim and M. Viberg, "Two Decades of Array Signal Processing Research", *IEEE Signal Processing Mag.* pp. 67-94, July, 1996.
- [4] H. Krim and M. Viberg, "Sensor Array Signal Processing: The Parameter Estimation Approach", *IEEE Sig. Proc. Mag.*, October, 1995.
- [5] R.T. Compton, "Adaptive Antennas: Concept and Performance", *Prentice Hall*, 1988.
- [6] P.W. Howells, "Intermediate frequency sidelobe canceller", *Technical report, U.S. Patent 3202990*, May 1959.
- [7] S. Applebaum, "Adaptive arrays," *IEEE Trans. Antennas & Propagat.* vol. AP-24, pp. 585-598, 1976.
- [8] B. Widrow and M. Hoff, "Adaptive switch circuit," in *IRE WESCOM, Conv. Rec., Part 4*, pp. 96-104, 1960.
- [9] O. Frost III, "An algorithm for linearly constrained adaptive array processing," *Proc. IEEE*, vol. 60, pp. 926-935, Aug. 1972.
- [10] L. Brook and I. Reed, "Equivalence of the likelihood ratio processor, the maximum signal- to-noise ratio filter, and the Wiener filter," *IEEE Trans. Aerosp. Electron. Syst.*, vol. 8, pp. 690-692, 1972.
- [11] J. Capon, "High resolution frequency wavenumber spectrum analysis," *Proc. IEEE*, vol. 57, pp. 1408-1418, Aug. 1969.
- [12] I. Reed, J Mallet, and L. Brennen, "Rapid convergence rate in adaptive arrays," *IEEE Trans. Aerosp. Electron. Syst.*, vol. AES-10, pp. 853-863, Nov. 1974.

- [13] J. Litva and T.K. Lo, "Digital beamforming in wireless communications", *Artech House Publishers*, 1996.
- [14] R. Monzingo and T. Miller, "Introduction to Adaptive Arrays, *John Wiley & Sons*, 1980.
- [15] L.C. Godara, "Error analysis of optimal antenna array processors," *IEEE Trans. Aerosp. Electron. Syst.*, vol. AES-22, pp. 395-409, 1986.
- [16] A.F. Naguib, "Adaptive antennas for CDMA wireless networks", *Ph.D. Dissertation, Stanford University*, 1996.
- [17] J. Munier and G. Delisle, "Spatial analysis in passive listening using adaptive techniques," *Proc. IEEE*, vol. 75, pp. 1458-1471, Aug. 1987.
- [18] J. Gobert, "Adaptive beam weighting," *IEEE Trans. Antennas & Propagat.* vol. AP-24, pp.744-749, 1976.
- [19] K. Takao and T. Ishizaki, "Constraints of the output power minimization adaptive array for broadband desired signal," *Trans. Inst. Electr. Commun. Eng. Jpn. B*, vol. J68-B, pp. 411-418, 1985.
- [20] E. Chong and S. Zak, "An Introduction to Optimization", *Wiley & Son Inc*, pp. 351-358, New York, 1996.
- [21] J. Winter, "Adaptive antenna for wireless systems", *Tutorial in Globecom 98*, Sydney, 1998.
- [22] K. Hugl et al. "Downlink Performance of Adaptive Antennas with Null Broadening", in *Proc. IEEE VTC'99*, Houston, USA, May, 1999.
- [23] J. Goldberg and J. Fonollosa, "Downlink beamforming for spatially distributed sources in cellular mobile communications". *Elsevier Science Signal Processing Journal*, vol. 65, pp. 181-197, 1998.

- [24] R. Chesarek, E. Drucker, "Signal feed matrix amplifier reduction system and method", *United States Patent No 5,917,371*. Dated: 29 June 1999
- [25] R. J. Mailloux, "Phased Array Antenna Handbook", *Artech House*, Dec. 1993.
- [26] T. Nguyen, M. Faulkner, "Null depth trade off for output power reduction in adaptive antenna array", in Proc. IEEE WPMC2000, Bangkok, Thailand, 2000.

APPENDIX

The copy of the paper published in the **IEEE International Symposium on Wireless and Personal Multimedia Communications – Bangkok 2000**

NULL DEPTH TRADE OFF FOR POWER REDUCTION IN ADAPTIVE ANTENNA ARRAYS

Tuan Nguyen, Mike Faulkner
Advanced Communications Technologies, Ltd. and
School of Communications and Informatics
Victoria University of Technology.
tuann@adcomtech.net mf@cabsav.vu.edu.au

Abstract

Adaptive antenna arrays have been used to form a time-varying beam pattern in order to minimise the co-channel interference. The performance of the adaptive array degrades when the separation angle between the desired user and the interferer's direction is small, therefore the handover is unavoidable. This paper presents a technique that can be used to reduce the separation angle between the desired user and the co-channel interferer in order to avoid unnecessary handover. The technique is based on an optimisation process, which trades off the null depth to reduce the power transmitted in the direction of the main lobe of the radiation beam pattern and that allows the interferer to come closer to the desired user. The narrower the separation angle the more traffic that can be handled by the base station and the less handovers are needed.

1. Introduction

Adaptive antenna arrays or "Smart antennas" are a promising solution for the problem of capacity demand. Adaptive antenna arrays at the base station demonstrate crucial advantages over conventional antennas due to their ability to form the main beam toward the desired user and nulls towards the interferers. However, when the null direction is too close to the desired user direction, the main lobe is shifted away from the direction of the desired user and increases drastically. The adjacent side lobes are also pulled up very high. The resulting beam pattern will cause serious inter-cell interference, which can only be avoided by forcing a handover. This phenomenon makes adaptive arrays incapable of forming an appropriate beam whenever the separation angle is small. Figure 1 shows the growth of the main lobe when the interference source approaches the desired user's direction. The plots of the magnitude of the tap weights of a uniform linear array, which are estimated by a zero-forcing beamformer, indicate the increase in transmit power required when null steering is added to beam steering of the main lobe (Figure 2). The magnitudes of the outermost taps increase drastically when the separation angle decreases to zero. This indicates the variation range of the outermost taps of the array is much greater than the inner taps. Therefore, the power distribution at the array taps is greatly nonuniform. This paper addresses the problem and proposes a novel method to improve the performance of

adaptive arrays in such situations by reducing the outer tap weights.

with SDMA (Space Division Multiple Access) applied on top of current TDMA (Time Division Multiple Access) or CDMA (Code Division Multiple Access), the traffic in the cell increases several fold [1]. However, the number of users that can be served simultaneously by the base station in SDMA depends on the "angular resolution" of the array (i.e. the minimum separation angle between any two co-channel users at which the array can still form an appropriate beam without excessive power emissions). The problem tackled in this article can help adaptive arrays to be used more efficiently in SDMA by increasing the "angular resolution".

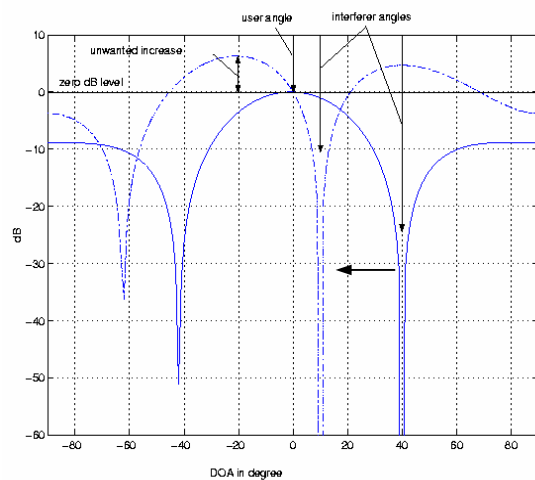


Figure 1. The beam patterns of a 3-element linear array using zero-forcing beamforming. The AOA (angle of arrival) of the desired user is at 0° (broadside angle) and the interferer is moving from 40° to 10° . The overshoot of the main lobe is approximately 8 dB.

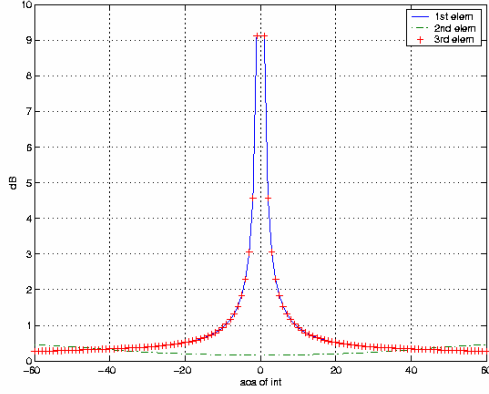


Figure 2. The variation of magnitude of the taps of the same array (zero forcing beamformer) when the desired user AOA is fixed at 0° and the interferer AOA (null position) swings from -90° to $+90^\circ$. (note that the 1st and the 3rd tap have the same magnitude and increase tremendously when the separation angle becomes small)

2. Zero-forcing beamformer and its nulling capability

Adaptive arrays can be equipped with different kinds of adaptive algorithms. These algorithms differ from one another by the adaptive criteria, the convergence speed, the sensitivity to errors, and the complexity. In the uplink, the adaptive array at the base station receives signals including the desired signal, cochannel interference and multipath copies of them. The AOAs (angle-of-arrival) of signals can be determined by using appropriate signal detection methods [1]. Once the AOAs of the signals are known, a relevant beamforming algorithm can be used to boost the desired signal and suppress the unwanted interferers.

In the downlink, the tap weight can be obtained directly or indirectly from the uplink [2]. In FDD (Frequency Division Duplex) systems, the frequency difference and uncorrelated fading between uplink and downlink prevent the use of uplink antenna weights for the downlink. One practical method to overcome this problem is to utilise the directions of arrival estimated from the received uplink data to calculate the complex antenna weights. These weights can be used to form a pattern that concentrates the transmit power towards the desired user and minimises the transmitted power towards cochannel users in other cells or within the same cell in SDMA. The zero-forcing beamformer is most suitable for this case, or at least the zero-forcing beamformer can be used as a showcase to examine the performance of the array whenever the separation angle is small.

2.1 Zero-forcing beamformer

In the zero-forcing beamforming method, the optimum weight vector is basically a minimum

solution for a linear system, which is constrained by predetermined array responses at the desired and the cochannel users directions. The number of total users is assumed to be less than or equal the number of array elements. Consider an N -element linear uniform array with L signal sources. Assume that θ_1 is the AOA of the desired user where unity response is required and $\theta_2, \theta_3, \dots, \theta_L$ are AOAs of cochannel users where nulls are required. The steering vectors $\mathbf{a}(\theta_i) \ i=1,2,\dots,L$ are given by:

$$\mathbf{a}(\theta_i) = \begin{bmatrix} 1 & e^{j2\pi\frac{d}{\lambda}\sin\theta_i} & \dots & e^{j2(N-1)\pi\frac{d}{\lambda}\sin\theta_i} \end{bmatrix}^T \quad (68)$$

where d is the interelement spacing and λ is the wavelength of the carrier. The optimum weight vector for the zero-forcing beamformer, \mathbf{W}_z , is the solution of the following simultaneous equations:

$$\begin{cases} \mathbf{w}^H \mathbf{a}(\theta_1) = 1 \\ \mathbf{w}^H \mathbf{a}(\theta_2) = 0 \\ \dots \\ \mathbf{w}^H \mathbf{a}(\theta_L) = 0 \end{cases} \quad (69)$$

Using matrix notation, (2) becomes:

$$\mathbf{A}^H \mathbf{W}_z = \mathbf{f} \quad (70)$$

where $\mathbf{A} = [\mathbf{a}(\theta_1) \ \mathbf{a}(\theta_2) \ \dots \ \mathbf{a}(\theta_{L-1}) \ \mathbf{a}(\theta_L)]$ is the array manifold, consisting of all L steering vectors of L directional sources and $\mathbf{f} = [1 \ 0 \ \dots \ 0]^T$ is a constraint vector consisting of the array response at each source direction.

The $(\cdot)^T$ and $(\cdot)^H$ denote the transpose and conjugate transpose respectively. If $L=N$ (the number of users is equal to the number of array elements), assuming that all steering vectors are linearly independent, the matrix A is invertible and thus (70) has a unique solution shown in (47):

$$\mathbf{w}_z = \mathbf{A}^{-1} \mathbf{f} \quad (71)$$

If $L < N$ (the number of users is less than the number of array elements), the matrix A is noninvertible and (70) is overdetermined. Using *min norm* theorem, the minimum solution in this case is:

$$\mathbf{w}_z = \mathbf{A}(\mathbf{A}^H \mathbf{A})^{-1} \mathbf{f} \quad (72)$$

The drawback of the zero-forcing beamformer is its sensitivity to the direction of nulls.

2.2 Nulling capability

Zero-forcing beamformers form very narrow and deep nulls towards the estimated AOAs of

cochannel users. If the estimated null directions were inaccurate (a few degrees error) then the null depths in the real cochannel users directions decrease very fast (Figure 3) causing a decrease in the SIR (Signal-to-Interference-Ratio). Also in the practical urban scattering environment, angular spread (caused by refraction or reflection from surrounding objects) of up to 15° have been measured [3] and this results in null filling (i.e. forming shallow null) in the array radiation pattern. In these practical situations, one single perfect null can not absolutely reject the interference from being received or transmitted.

Therefore, a deliberate reduction of the null depth in order to improve the array performance in some situations is a wise choice as in practice the infinite nulls never occur.

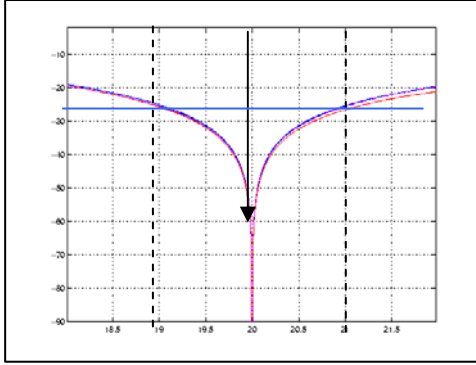


Figure 3. The single perfect null in 3-element array beam pattern. The null depth at 20° is infinity while the null depth at 19° and 21° is only -25 dB.

3. Output power reduction by changing the null depth

3.1 Global minimum of the output power surface

As mentioned in 2.1, the optimum weight of the zero forcing beamformer is the minimum solution of the linear system (45).

The array response at the angle θ can be defined as:

$$F = \mathbf{w}_z^H \mathbf{a}(\theta) = \sum_{i=1}^N w_i e^{j(i-1)\xi} \quad (73)$$

where $\xi = 2\pi \frac{d}{\lambda} \sin \theta$. The output power density of the array at the angle θ can be defined as:

$$P(\theta) = FF^H = \mathbf{w}_z^H \mathbf{a}(\theta) \mathbf{a}^H(\theta) \mathbf{w}_z \quad (74)$$

Therefore the total output power is the area under the curve $P(\theta)$:

$$P = \int_0^{2\pi} P(\theta) d\theta = \int_0^{2\pi} (\mathbf{w}_z^H \mathbf{a}(\theta) \mathbf{a}^H(\theta) \mathbf{w}_z) d\theta = \mathbf{w}_z^H \mathbf{w}_z \int_0^{2\pi} \mathbf{a}(\theta) \mathbf{a}^H(\theta) d\theta = C \sum_{i=1}^N |w_i|^2 \quad (75)$$

where C is a constant depending on the array geometric configuration. The coefficient C can be dropped without loss of generality and the total power P can be expressed as:

$$P = \|\mathbf{w}_z\|^2 = \mathbf{w}_z^H \mathbf{w}_z = \sum_{i=1}^N |w_i|^2 \quad (76)$$

Substituting (48) into (49) gives:

$$P = (\mathbf{A}(\mathbf{A}^H \mathbf{A})^{-1} \mathbf{f})^H \mathbf{A}(\mathbf{A}^H \mathbf{A})^{-1} \mathbf{f} = \mathbf{f}^H (\mathbf{A}^H \mathbf{A})^{-1} \mathbf{f} \quad (77)$$

If the constraint vector \mathbf{f} is modified then the output power will be changed accordingly. In the perfect nulling scheme (i.e. null depths are infinite) the constraint vector \mathbf{f} has the form:

$\mathbf{f} = [1 \ 0 \ \dots \ 0]^T$. If the components of the \mathbf{f} vector become non zero $\mathbf{f} = [f_1 \ f_2 \ \dots \ f_L]^T$ where $f_i = 1, f_i > 0$ ($i=2, \dots, L$) then the absolute value of f_i will determine the null depth. The system in (2) becomes:

$$\begin{cases} \mathbf{w}^H \mathbf{a}(\theta_1) = f_1 \\ \mathbf{w}^H \mathbf{a}(\theta_2) = f_2 \\ \dots \\ \mathbf{w}^H \mathbf{a}(\theta_L) = f_L \end{cases} \quad (78)$$

The output power, $P(\mathbf{f}) = \mathbf{f}^H (\mathbf{A}^H \mathbf{A})^{-1} \mathbf{f}$ which is a quadratic function of the constraint vector, \mathbf{f} , can be minimised with respect to \mathbf{f} . The optimisation problem can be expressed as:

$$\begin{aligned} &\text{minimize } P(\mathbf{f}) = \mathbf{f}^H (\mathbf{A}^H \mathbf{A})^{-1} \mathbf{f} \\ &\text{subject to } \begin{cases} f_1 = \delta_1 \\ 0 < f_2 \leq \delta_2 \\ \dots \\ 0 < f_L \leq \delta_L \end{cases} \end{aligned} \quad (79)$$

where: δ_i is the predetermined look direction response and $\delta_2, \dots, \delta_L$ are and null depths of the output pattern. The main idea of the null depth control technique is to find the optimum value of the components $0 < f_i < \delta_i$ ($i=2, \dots, L$) of the constraint vector \mathbf{f} in a certain region so that the output power P is minimum. Finding the general solution for this problem is rather difficult. The global minimum of the output power surface can be found using the *Kuhn-Tucker theorem* [4], will be mentioned in the next publication.

3.2 Local minimum of the output power surface.

One approach to null depth control is to find local minimum of the output power surface $P=g(\mathbf{f})$. In this approach we only try to reduce the depth of one null whose direction is closest to the look direction. In practice, the modification of one null may be effective enough. (52) can be simplified to:

$$\begin{aligned} & \text{minimize } P(\mathbf{f}) = \mathbf{f}^H (\mathbf{A}^H \mathbf{A})^{-1} \mathbf{f} \\ & \text{subject to } \begin{cases} f_1 = 1 \\ f_2 = \delta \\ \dots \\ f_L = 0 \end{cases} \end{aligned} \quad (80)$$

Now the task is to find the complex displacement $\delta = |\delta|e^{j\phi}$ so that P is minimised. The δ can be found by differentiation of the output power, P , with respect to $|\delta|$ as follows:

$$\frac{\partial P(\delta)}{\partial |\delta|} = 0 \quad (81)$$

Let $\mathbf{K} = (\mathbf{A}^H \mathbf{A})^{-1}$ so (81) becomes:

$$\begin{aligned} \frac{\partial P(\delta)}{\partial |\delta|} &= \frac{\partial (\mathbf{f}^H \mathbf{K} \mathbf{f})}{\partial |\delta|} \\ &= \frac{\partial \mathbf{f}^H}{\partial |\delta|} \mathbf{K} \mathbf{f} + \mathbf{f}^H \mathbf{K} \frac{\partial \mathbf{f}}{\partial |\delta|} = 0 \end{aligned} \quad (82)$$

the vector \mathbf{f} can be written as:

$$\mathbf{f} = [1, |\delta|e^{j\phi}, \mathbf{0}]^T \text{ and } \mathbf{f}^H = [1, |\delta|e^{-j\phi}, \mathbf{0}] \quad (83)$$

where $\mathbf{0} = [0 \dots 0]$ is a vector, which consists of $(L-2)$ zeros. The derivative of these vectors are:

$$\frac{\partial \mathbf{f}^H}{\partial |\delta|} = [0, e^{-j\phi}, \mathbf{0}] \text{ and} \quad (84)$$

$$\frac{\partial \mathbf{f}}{\partial |\delta|} = [0, e^{j\phi}, \mathbf{0}]^T :$$

substituting (56)-(84) into (82) yields:

$$\begin{aligned} [0, e^{-j\phi}, \mathbf{0}] \mathbf{K} [1, |\delta|e^{j\phi}, \mathbf{0}]^T + \\ [1, |\delta|e^{-j\phi}, \mathbf{0}] \mathbf{K} [0, e^{j\phi}, \mathbf{0}]^T = 0 \end{aligned} \quad (85)$$

(85) can be further simplified to:

$$\begin{aligned} e^{-j\phi} \mathbf{K}_{2,1 \dots L} [1, |\delta|e^{j\phi}, \mathbf{0}]^T + \\ [1, |\delta|e^{-j\phi}, \mathbf{0}] \mathbf{K}_{1 \dots L, 2} e^{j\phi} = 0 \end{aligned} \quad (86)$$

where $\mathbf{K}_{m,n}$ denotes the element of the matrix \mathbf{K} at the m -th row and n -th column.

$$e^{-j\phi} (\mathbf{K}_{2,1} + \mathbf{K}_{2,2} |\delta| e^{j\phi}) + \quad (87)$$

$$e^{j\phi} (\mathbf{K}_{1,2} + \mathbf{K}_{2,2} |\delta| e^{-j\phi}) = 0$$

$$e^{-j\phi} \mathbf{K}_{2,1} + 2\mathbf{K}_{2,2} |\delta| + e^{j\phi} \mathbf{K}_{1,2} = 0 \quad (88)$$

$$|\delta| = -\frac{e^{j\phi} \mathbf{K}_{1,2} + e^{-j\phi} \mathbf{K}_{2,1}}{2\mathbf{K}_{2,2}} \quad (89)$$

Equation (89) shows that there exists a δ at which the output power has an extremum (either minimum or maximum). This extremum of

output power, P , can be proven to be minimum by testing the second order derivative of P . However, this solution is trivial because the null depth is the same as what we would get from beam forming without null steering at all.

In practical situations the null depth can be set in advance using the minimum requirement for the SIR. This means that the $|\delta|$ can be set so that the null depth is greater than a certain level, the minimisation of P can be achieved by varying the angle ϕ . The differential equation is similar to (14)

$$\frac{\partial P(\phi)}{\partial \phi} = 0 \quad (90)$$

(23) can be expanded like (17) to produce:

$$\begin{aligned} \frac{\partial P(\phi)}{\partial \phi} &= \frac{\partial (\mathbf{f}^H \mathbf{K} \mathbf{f})}{\partial \phi} \\ &= \frac{\partial \mathbf{f}^H}{\partial \phi} \mathbf{K} \mathbf{f} + \mathbf{f}^H \mathbf{K} \frac{\partial \mathbf{f}}{\partial \phi} = 0 \end{aligned} \quad (91)$$

the partial derivative provides:

$$\frac{\partial \mathbf{f}^H}{\partial \phi} = -j[0, |\delta|e^{-j\phi}, \mathbf{0}] \quad (92)$$

$$\text{and } \frac{\partial \mathbf{f}}{\partial \phi} = j[0, |\delta|e^{j\phi}, \mathbf{0}]^T :$$

substituting (56)-(57) into (55) yields:

$$-j[0, e^{-j\phi}, \mathbf{0}] \mathbf{K} [1, |\delta|e^{j\phi}, \mathbf{0}]^T + \quad (93)$$

$$j[1, |\delta|e^{-j\phi}, \mathbf{0}] \mathbf{K} [0, e^{j\phi}, \mathbf{0}]^T = 0$$

$$-|\delta|e^{-j\phi} \mathbf{K}_{2,1 \dots L} [1, |\delta|e^{j\phi}, \mathbf{0}]^T + \quad (94)$$

$$[1, |\delta|e^{-j\phi}, \mathbf{0}] \mathbf{K}_{1 \dots L, 2} |\delta|e^{j\phi} = 0$$

where $\mathbf{K}_{i,j}$ denotes the i -th row, j -th column element of matrix \mathbf{K}

$$-e^{-j\phi} (\mathbf{K}_{2,1} + \mathbf{K}_{2,2} |\delta| e^{j\phi}) + \quad (95)$$

$$e^{j\phi} (\mathbf{K}_{1,2} + \mathbf{K}_{2,2} |\delta| e^{-j\phi}) = 0$$

$$-e^{-j\phi} \mathbf{K}_{2,1} + e^{j\phi} \mathbf{K}_{1,2} = 0 \quad (96)$$

$$\phi = \frac{1}{2} \arg \left\{ \frac{\mathbf{K}_{2,1}}{\mathbf{K}_{1,2}} \right\} = \arg \left\{ \mathbf{K}_{2,1} \right\} \text{ since} \quad (97)$$

$$\mathbf{K}_{2,1} = \mathbf{K}_{1,2}^*$$

In order to prove that this is a minimum point, we can use the second order derivative of P :

$$\frac{\partial P^2(\phi)}{\partial \phi^2} = \quad (98)$$

$$\frac{\partial}{\partial \phi} (-|\delta|e^{-j\phi}\mathbf{K}_{2,1} + 2\mathbf{K}_{2,2}|\delta|^2 + |\delta|e^{j\phi}\mathbf{K}_{1,2})$$

$$= j|\delta|(e^{-j\phi}\mathbf{K}_{2,1} + e^{j\phi}\mathbf{K}_{1,2})$$

assuming that: $K_{2,1} = |k|e^{j\gamma}$ and

$K_{1,2} = |k|e^{-j\gamma}$ then (31) can be written as:

$$\phi = \gamma \pm n\pi \text{ where } n=0,1,2\dots \quad (99)$$

and (32) becomes:

$$\frac{\partial P^2(\phi)}{\partial \phi^2} = \quad (100)$$

$$\frac{\partial}{\partial \phi} \{j|\delta||k|(e^{-j\phi}e^{j\gamma} + e^{j\phi}e^{-j\gamma})\} =$$

$$\begin{cases} 2|\delta||k| > 0 & \text{if } \phi = \gamma \pm 2n\pi \\ -2|\delta||k| < 0 & \text{if } \phi = \gamma \pm 2(n+1)\pi \end{cases}$$

Equation (33) shows that there exists a phase angle, $\phi = \gamma \pm 2n\pi$ of the complex displacement δ at which the output power P is minimum. From this point, it is necessary to emphasise that with the predetermined null depth, it is possible to reduce the output power by varying the phase of the complex displacement, δ .

3.3 Geometrical interpretation

The solution of (12) essentially determines the shortest vector, \mathbf{w}_z , which satisfies all the constraints expressed in the linear system (11). A geometrical interpretation is shown in Figure 4, for a 3-element array and two signal sources (one desired user and one interferer) i.e $N=3, L=2$. In this particular scenario, \mathbf{w}_z is a vector perpendicular to the solid line PQ , which is the intersection of two hyperplanes, $\mathbf{w}_z\mathbf{a}(\theta_1)=1$, and $\mathbf{w}_z\mathbf{a}(\theta_2)=0$. When the constraint plane, $\mathbf{w}_z\mathbf{a}(\theta_1)=1$, containing the origin of the coordination system, is translated away from its original position, PQ becomes $P'Q'$ and the weight vector, \mathbf{w}_z becomes \mathbf{w}'_z . \mathbf{w}'_z has a new magnitude and orientation, and as a result, the downlink array output power, $P=||\mathbf{w}_z||^2$, has changed. The objective of the translation is to determine a value of $|\delta|$ for which the output power, P , is minimised regardless of the null depth. The magnitude of displacement, $|\delta|$, represents a finite null depth. The displacement of δ which gives the minimum output power is in fact the weight of the zero-forcing beamformer with only one desired user and no interferer. Obviously this is a trivial solution as mentioned above.

In order to avoid a trivial solution, the null depth must be given priority, i.e. $|\delta|$ is given in advance. Because, in a practical situation the minimum requirement for the SIR is normally predetermined. In this case: the constraint hyperplane, $\mathbf{w}_z\mathbf{a}(\theta_2)=0$, is translated a distance equal to $|\delta|$ and then rotated by the angle, ϕ , as described in equation (23). This process is shown in the Figure 5:

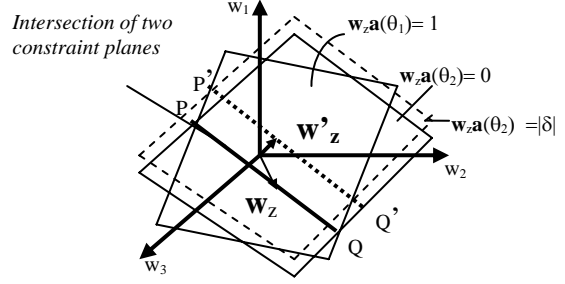


Figure 4 : The change of the optimal zero-forcing weight when the constraint plane is translated in a parallel direction.

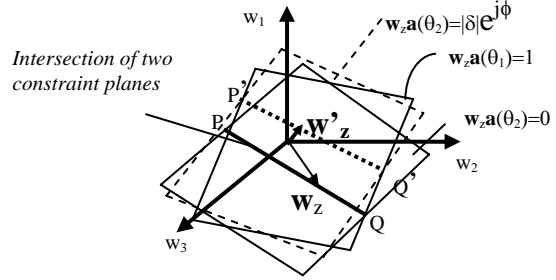


Figure 5 : The change of the optimal zero-forcing weight when the constraint plane is translated and rotated.

4. Numerical verification and simulation results

A numerical evaluation of the output power versus the null depth, $|\delta|$, and the phase, ϕ , was carried out in order to verify the validity of the null depth control technique. A 3-element array with half-wave length interelement spacing has been used. The channel has two signal sources (desired user and cochannel user) located at 0° and 10° respectively. Figure 6(a) shows the output power surface of the array versus amplitude and phase of the complex displacement, δ . The lowest point represents a minimum output power expected without forming a null (which is a trivial solution). This surface forms a valley along the axes of the phase, ϕ . The cross-sections of the power surface are shown in Figure 6(b). The lowest points of the cross-section represents

the output power at ϕ_{opt} for different null depth $|\delta|=0, 0.25, 0.75, 1$.

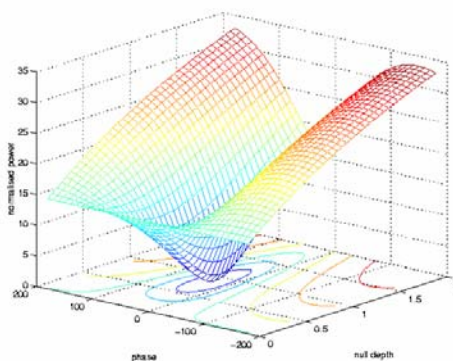
Figure 7 shows the relationship between the minimum out put power and null depth for different separation angles ($\theta_s=5^\circ, 10^\circ, 15^\circ, 20^\circ$). The same array as in the previous example has been investigated. The plots indicate that when the separation angle is small, the null depth control can save a significant amount of transmit power. (approximately 6dB for the case of 5° separation angle and -10dB null depth).

5. Conclusion

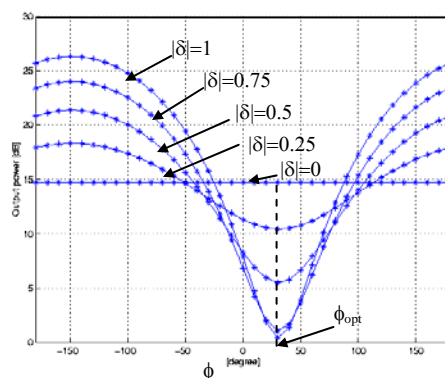
A null depth adjustment technique, using a modified zero-forcing beamforming was presented. This technique can be used to control the increase in the adaptive array power due to a small separation angle between a desired user and a cochannel user. The technique was analysed and verified by the computer simulation for the CDF of the output power of a 3-element array. Applying this technique reduces the chance of power overload at the array element and reduces the interference to the other cells and consequently allows more traffic being served in the cells.

REFERENCES

- [1] H. Krim and M. Viberg, "Two Decades of Array Signal Processing Research", IEEE Signal Processing Mag., pp. 67-94, July, 1996.
- [2] L.C. Godara, "Applications of Antenna Array to Mobile Communications, Part II: Beamforming and Directions -of - Arrival Considerations", IEEE Proceedings vol. 85, No. 8, pp. 1193-1245, August, 1997.
- [3] K. Hugi et al. "Downlink Performance of Adaptive Antennas with Null Broadening", Proc. IEEE VTC'99, pp. , Houston, USA, May, 1999.
- [4] E. Chong and S. Zak, "An Introduction to Optimisation", Wiley & Son Inc, pp. 351-358, New York, 1996.



(a)



(b)

Figure 6. (a) The output power surface of the 3-element array with respect to magnitude and phase of the displacement δ .

(b) The cross-sectional of the power surface at different values of $|\delta|$.

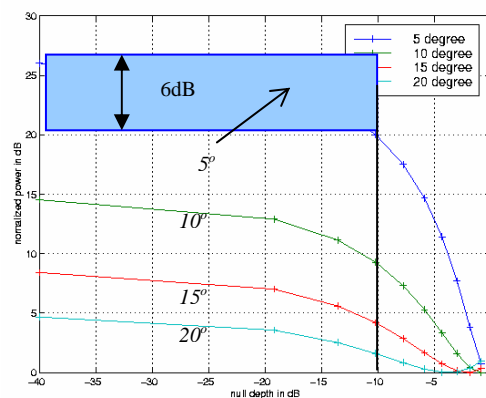


Figure 7. The output power curve vs. the null depth for different separation angle of $5^\circ, 10^\circ, 15^\circ, 20^\circ$